

# Causal particle detectors and topology

Paul Langlois\*

*School of Mathematical Sciences, University of Nottingham  
Nottingham NG7 2RD, UK*

July 4, 2018

## Abstract

We investigate particle detector responses in some topologically non-trivial spacetimes. We extend a recently proposed regularization of the massless scalar field Wightman function in 4-dimensional Minkowski space to arbitrary dimension, to the massive scalar field, to quotients of Minkowski space under discrete isometry groups and to the massless Dirac field. We investigate in detail the transition rate of inertial and uniformly accelerated detectors on the quotient spaces under groups generated by  $(t, x, y, z) \mapsto (t, x, y, z + 2a)$ ,  $(t, x, y, z) \mapsto (t, -x, y, z)$ ,  $(t, x, y, z) \mapsto (t, -x, -y, z)$ ,  $(t, x, y, z) \mapsto (t, -x, -y, z + a)$  and some higher dimensional generalizations. For motions in at constant  $y$  and  $z$  on the latter three spaces the response is time dependent. We also discuss the response of static detectors on the  $\mathbb{RP}^3$  geon and inertial detectors on  $\mathbb{RP}^3$  de Sitter space via their associated global embedding Minkowski spaces (GEMS). The response on  $\mathbb{RP}^3$  de Sitter space, found both directly and in its GEMS, provides support for the validity of applying the GEMS procedure to detector responses and to quotient spaces such as  $\mathbb{RP}^3$  de Sitter space and the  $\mathbb{RP}^3$  geon where the embedding spaces are Minkowski spaces with suitable identifications.

## 1 Introduction

In this paper we investigate particle detector models in topologically non-trivial spacetimes. The aims are two-fold. Firstly we discuss a recent paper by Schlicht [1] in which the usual regularization procedure for the positive frequency Wightman function [2] is criticized in the context of particle detectors in Minkowski space and an alternative is proposed. We extend the regularization introduced by Schlicht to Minkowski space of arbitrary dimension, to the massive scalar field, to automorphic fields and to the massless Dirac field. Secondly we present detector responses on certain topologically non-trivial spacetimes, with the aim of investigating the effect of the non-trivial topology on the Unruh and Hawking effects [3, 4].

Particle detector models in the context of quantum field theory in curved space-time were first considered by Unruh [3], who proved his now famous result that a uniformly accelerated detector in Minkowski space responds as in a thermal bath at the temperature  $T = a/(2\pi)$ . Unruh's model consists of a particle in a box coupled to the quantum field. The detection of a particle is indicated by the excitation of the

---

\*Electronic Address: pmxpp1@nottingham.ac.uk

detector by the field. Shortly after Unruh, DeWitt [5] considered a simpler model consisting of a monopole moment operator coupled to the field along the detector's worldline. This is the model subsequently considered most in the literature. Good reviews of the early literature are found in [2, 6].

In the usual derivation of the Unruh effect using DeWitt's monopole detector the detection is considered in the asymptotic regions where the detector is switched on in the infinite past and off in the infinite future. Recently Schlicht [1] has considered the case of a detector switched on in the infinite past but read at a finite time  $\tau$  and has highlighted the importance of choosing a suitable regularization of the Wightman function. In particular Schlicht shows that a naive  $i\epsilon$ -prescription, as is usually used in the asymptotic case [2], for a uniformly accelerated detector, leads to a  $\tau$ -dependent and thus presumably unphysical response. Schlicht proposes an alternative regularization procedure by considering the monopole detector as the limit of a rigid detector with spatial extension. The monopole moment operator is coupled to the field via a smeared field operator where the smearing is performed in the detector's rest frame. He recovers the usual responses in the case of inertial and uniformly accelerated motion. He further considers a trajectory which smoothly interpolates between the two obtaining physically reasonable results.

We begin here in section 2 by extending the regularization introduced by Schlicht [1] to a massless scalar field in Minkowski space of arbitrary dimension. We recover the expected responses for inertial and uniformly accelerated detectors. In section 3 we extend the regularization further to a massive scalar field in four-dimensional Minkowski space.

In section 4 we consider detectors on quotient spaces of Minkowski space under certain discrete isometry groups, via detectors coupled to automorphic fields [7, 8] in Minkowski space. We begin by extending Schlicht's regularization to these quotient spaces. We then present a number of responses on a number of specific spacetimes and trajectories of interest. Our main motivation is to investigate the effect of non-trivial topology on the Hawking and Unruh effects. In particular our interest lies in the (non)-thermality of the Hartle-Hawking-like vacuum on the  $\mathbb{RP}^3$  geon black hole spacetime as seen by static observers [9, 10] and the Euclidean-like vacuum state on  $\mathbb{RP}^3$  de Sitter space [11]. We consider inertial and uniformly accelerated observers on the quotient spaces of Minkowski space under the involutions  $J_0 : (t, x, y, z) \mapsto (t, x, y, z + 2a)$  and  $J_- : (t, x, y, z) \mapsto (t, -x, -y, z + a)$  (denoted here by  $M_0$  and  $M_-$  respectively), in the Minkowski-like vacuum states.  $M_0$  and  $M_-$  may be used to model the Hawking effect on the Kruskal manifold and the  $\mathbb{RP}^3$  geon respectively [9, 10] and to illustrate the affect of the topology on the Unruh effect in flat spacetimes. We also consider inertial and uniformly accelerated detectors on Minkowski space with an infinite flat plane boundary, on a conical spacetime and on some higher dimensional generalizations.

For motions perpendicular to the boundary the boundary spacetime serves as a simpler model in which many of the features of the responses on  $M_-$  are present. Further the responses are interesting in their own right. The boundary spacetime with Dirichlet boundary conditions has been used to investigate the detection of negative energy densities [12] and may have relevance to the quantum inequalities program [13–20]. In the literature the time independent response of detectors with motion parallel to the boundary has been considered [12, 21]. We present the time

dependent response of detectors with motion perpendicular to the boundary.

The conical spacetime may be considered as the spacetime outside an infinite, straight and zero radius cosmic string. The response of detectors travelling parallel to such a string has been considered in [22,23]. We present the response of a detector approaching the string.

In section 5 we extend the model of Schlicht to the massless Dirac field both in Minkowski space and in the quotient spaces using the automorphic field theory. For inertial and uniformly accelerated detectors we recover the expected results for the transition rate and power spectrum [6] on Minkowski space, and we discuss these detectors on  $M_0$ . Further we address the issue as to whether or not such a detector can distinguish the two spin structures on  $M_0$  and  $M_-$  [10]. Unfortunately on  $M_-$  we find that our model is not sensitive to the spin structure for any motions at constant  $y$  and  $z$ .

Finally the responses on the boundary and conical spacetimes and the higher dimensional generalizations of section 4 are relevant also for the responses of static detectors on the  $\mathbb{RP}^3$  geon and inertial detectors in  $\mathbb{RP}^3$  de Sitter space, via their associated global embedding Minkowski spaces (GEMS) [24]. Although until now the GEMS procedure has only been applied to kinematical arguments we expect that at least in some cases the response of detectors in the original curved spaces and the corresponding ones in their GEMS should be related in some way. In section 6 we begin with a brief review of the GEMS literature. We then present an embedding of the Kruskal manifold in a 7-dimensional Minkowski space, introduced in [25], and a related embedding of the  $\mathbb{RP}^3$  geon in a 7-dimensional Minkowski space with identifications. The Hawking temperature as seen by a static observer on the Kruskal manifold is obtained by kinematical arguments from the related Unruh temperature of the observer in the embedding space. We then argue that on the  $\mathbb{RP}^3$  geon the response of a static detector, in the Hartle-Hawking-like vacuum, should be related to the response of the associated Unruh observer in the embedding space, in the Minkowski-like vacuum. This response is given by results in section 4.

In section 7 we consider inertial detectors in de Sitter and  $\mathbb{RP}^3$  de Sitter space. We begin by introducing a causal detector and calculating the response of a uniformly accelerated detector in de Sitter space, in the Euclidean vacuum, in a causal way. The thermal result agrees with the literature [26]. Next we consider the response of an inertial detector in  $\mathbb{RP}^3$  de Sitter space, in the Euclidean-like vacuum with the motion perpendicular to the distinguished foliation [11]. The response is seen to be identical to that of the uniformly accelerated detector on four-dimensional Minkowski space with infinite plane boundary found in section 4. On de Sitter and  $\mathbb{RP}^3$  de Sitter space we also consider the response of detectors via their 5-dimensional GEMS. The thermal response in de Sitter space has been given before [26]. The GEMS calculation on  $\mathbb{RP}^3$  de Sitter space is a particularly interesting one as we are able to present the calculation both in the curved space and in the embedding space. It is found that the responses are qualitatively very similar. This case should therefore be very useful in assessing the validity of applying the GEMS procedure to cases involving quotient spaces and time dependent detector responses.

We work throughout in natural units  $\hbar = c = G = 1$  and with metric signature  $(+, -, \dots, -)$ . In  $d$ -dimensional Minkowski space, the spatial  $(d - 1)$ -vectors are denoted by bold face characters  $\mathbf{x} \in \mathbb{R}^{d-1}$  with  $\cdot$  the usual scalar product in  $\mathbb{R}^{d-1}$ ,

while  $d$ -vectors (used occasionally) are given by an italic script  $x$  with  $x \cdot y = g_{\mu\nu} x^\mu y^\nu$ , where  $g_{\mu\nu}$  is the Minkowski metric.

## 2 Causal detector in $d$ dimensions

In this section we introduce DeWitt's monopole detector [5]. We discuss the use of spatial sampling functions to regularize the correlation function and extend the regularization in [1], using a Lorentzian sampling function, to  $d$ -dimensional Minkowski space  $M$ ,  $d > 2$ .<sup>1</sup>

The model is that of a monopole detector, moving along a prescribed classical trajectory in  $M$  and coupled to a massless scalar field  $\phi$ . The field has Hamiltonian  $H_\phi$ , and satisfies the massless Klein-Gordon equation. The free field operator is expanded in terms of a standard complete set of orthonormal solutions to the field equation as

$$\phi(t, \mathbf{x}) = \frac{1}{(2\pi)^{(d-1)/2}} \int \frac{d^{d-1}k}{(2\omega)^{1/2}} \left( a(\mathbf{k}) e^{-i(\omega t - \mathbf{k} \cdot \mathbf{x})} + a^\dagger(\mathbf{k}) e^{i(\omega t - \mathbf{k} \cdot \mathbf{x})} \right), \quad (1)$$

where  $(t, x_1, x_2, \dots, x_{d-1})$  are usual Minkowski coordinates and, in the massless case,  $\omega = |\mathbf{k}|$ . The field is quantized by imposing, for the creation and annihilation operators, the usual commutation relations

$$[a(\mathbf{k}), a^\dagger(\mathbf{k}')] = \delta^{d-1}(\mathbf{k} - \mathbf{k}'). \quad (2)$$

The Minkowski vacuum  $|0\rangle$  is the state annihilated by all the annihilation operators.

The detector is a quantum mechanical system with a set of energy eigenstates  $\{|0_D\rangle, |E_i\rangle\}$ . It moves along a prescribed classical trajectory  $t = t(\tau)$ ,  $\mathbf{x} = \mathbf{x}(\tau)$ , where  $\tau$  is the detector's proper time, and it couples to the scalar field via the interaction Hamiltonian

$$H_{\text{int}} = cm(\tau)\phi(\tau), \quad (3)$$

where  $c$  is a (small) coupling constant and  $m(\tau)$  is the detector's monopole moment operator [5]. The evolution of  $m(\tau)$  is given by

$$m(\tau) = e^{iH_D\tau} m(0) e^{-iH_D\tau}. \quad (4)$$

Suppose that at time  $\tau_0$  the detector and field are in the product state  $|0, E_0\rangle = |0\rangle|E_0\rangle$ , where  $|E_0\rangle$  is a detector state with energy  $E_0$ . The probability that at time  $\tau_1 > \tau_0$  the detector is found in an excited state  $|E_1\rangle$ , regardless of the final state of the field, is, to first order in perturbation theory

$$\sum_{\psi} |\langle \psi, E_1 | 0, E_0 \rangle|^2 = c^2 |\langle E_1 | m(0) | E_0 \rangle|^2 \int_{\tau_0}^{\tau_1} d\tau \int_{\tau_0}^{\tau_1} d\tau' e^{-i(E_1 - E_0)(\tau - \tau')} \langle 0 | \phi(\tau) \phi(\tau') | 0 \rangle. \quad (5)$$

---

<sup>1</sup>The two-dimensional case may be dealt with in a similar way with the added complication of the well known infrared divergence [27]. The correlation function contains an infinite constant term, which can be shown to not contribute to the response provided that the detector is switched on and off smoothly. We shall not spell out the two-dimensional case further here.

This expression has two parts. The sensitivity  $c^2|\langle E_1|m(0)|E_0\rangle|^2$  depends only on the internal details of the detector and is not considered hereafter. The “response function”

$$F_{\tau_0, \tau_1}(\omega) = \int_{\tau_0}^{\tau_1} d\tau \int_{\tau_0}^{\tau_1} d\tau' e^{-i\omega(\tau-\tau')} \langle 0|\phi(\tau)\phi(\tau')|0\rangle , \quad (6)$$

where  $\omega = E_1 - E_0$  ( $\omega > 0$  for excitations and  $\omega < 0$  for de-excitations), does not depend on the internal details of the detector and so is common for all such detectors.

We now follow Schlicht [1] and change coordinates to  $u = \tau$ ,  $s = \tau - \tau'$  for  $\tau' < \tau$  and  $u = \tau'$ ,  $s = \tau' - \tau$  for  $\tau' > \tau$  and then differentiate with respect to  $\tau_1$  to obtain an expression for the “transition rate”

$$\dot{F}_{\tau_0, \tau}(\omega) = 2 \int_0^{\tau - \tau_0} ds \operatorname{Re} (e^{-i\omega s} \langle 0|\phi(\tau)\phi(\tau-s)|0\rangle) , \quad (7)$$

where we have written  $\tau_1 = \tau$ . The transition rate is clearly causal in the sense that it does not depend on the state of motion of the detector after time  $\tau$  but only on times  $\tau_0 < \tau' < \tau$  which label the past motion of the detector.

The correlation function  $\langle 0|\phi(x)\phi(x')|0\rangle$  in (7) is the positive frequency Wightman function which can be obtained from the expansion (1)

$$\langle 0|\phi(x)\phi(x')|0\rangle = \frac{1}{(2\pi)^{d-1}} \int \frac{d^{d-1}k}{2\omega} e^{-i\omega(t-t')+i\mathbf{k}\cdot(\mathbf{x}-\mathbf{x}')} . \quad (8)$$

The integrals in (8) may be performed by first transforming to hyperspherical coordinates in  $\mathbf{k}$ -space. The  $|\mathbf{k}|$  integral requires regularization due to the usual ultraviolet divergences found in quantum field theory.

The fundamental observation of reference [1] is that if we regularize the divergences in (8) using the usual  $i\epsilon$ -prescription, that is we introduce the cut-off  $e^{-\epsilon\omega}$ , and then use it to compute the transition rate (7) on a uniformly accelerated world-line with acceleration  $1/\alpha$  and proper time  $\tau$ ,

$$\begin{aligned} t &= \alpha \sinh(\tau/\alpha) , \\ x &= \alpha \cosh(\tau/\alpha) , \end{aligned} \quad (9)$$

with the detector switched on in the infinite past,  $\tau_0 = -\infty$ , we obtain a time dependent and apparently unphysical result, instead of the expected time independent thermal result (see e.g. [2,5]). Schlicht shows this in four dimensions by specific numerical and analytic calculations, and the general  $d$  case follows similarly.

Schlicht’s proposal is to consider an alternative regularization where the monopole detector is considered as the limit of a detector with spatial extension which is rigid in the detector’s rest frame. Instead of the interaction Hamiltonian (3) with  $\phi(\tau) = \phi(x(\tau))$  we consider (3) with the monopole moment operator coupled to the smeared field

$$\phi(\tau) = \int d^{d-1}\xi W_\epsilon(\xi) \phi(x(\tau, \xi)) , \quad (10)$$

where  $(\tau, \xi)$  are Fermi coordinates (see e.g. [28]) and  $W_\epsilon(\xi)$  is a window sampling function of characteristic length  $\epsilon$ . In effect (10) introduces a cut-off at short distances of the order of  $\epsilon$  in size.

We may choose a window function with infinite support, such as that used in [1], if the window function decreases sufficiently rapidly at large distances. Or we may consider a detector of truly finite extent with the use of a window function with compact support. We require the window function to be normalised as

$$\int d^{d-1}\xi W_\epsilon(\xi) = 1 , \quad (11)$$

so that smearing a constant function will return that constant value. We also require the window function to approximate the  $(d-1)$ -dimensional Dirac  $\delta$  function, so that in the limit as  $\epsilon$  tends to 0, (10) formally gives the field value  $\phi(x(\tau))$ . The window function hence satisfies  $W_\epsilon(\xi) \approx 0$  for  $|\xi| >> \epsilon$  and  $W_\epsilon(\xi) \propto \epsilon^{-(d-1)}$  for  $|\xi| << \epsilon$ .

We now extend Schlicht's regularization of the Wightman function (8) to  $d$ -dimensional Minkowski space. Although a large number of different window functions could be considered, the one chosen in [1] seems to be the easiest for obtaining a closed expression for the Wightman function on an arbitrary trajectory.

The  $d$ -dimensional analogue of the window function considered in [1] is

$$W_\epsilon(\xi) = \frac{\Gamma[d/2]}{\pi^{d/2}} \frac{\epsilon}{(\xi^2 + \epsilon^2)^{d/2}} . \quad (12)$$

(12) is sometimes referred to as a Lorentzian window or sampling function. It approximates a  $(d-1)$ -dimensional Dirac  $\delta$  function and is suitably normalized.

Using (10) and (12), we find

$$\begin{aligned} \langle 0 | \phi(\tau) \phi(\tau') | 0 \rangle &= \frac{1}{(2\pi)^{d-1}} \int \frac{d^{d-1}k}{2\omega} \int d^{d-1}\xi W_\epsilon(\xi) e^{-i(\omega t(\tau, \xi) - \mathbf{k} \cdot \mathbf{x}(\tau, \xi))} \\ &\quad \times \int d^{d-1}\xi' W_\epsilon(\xi') e^{i(\omega t(\tau', \xi') - \mathbf{k} \cdot \mathbf{x}(\tau', \xi'))} . \end{aligned} \quad (13)$$

The integrals over  $\xi$  and  $\xi'$  in (13) may be performed by transforming to hyperspherical coordinates and with analogous arguments to those used in [1] in four dimensions we find

$$\langle 0 | \phi(\tau) \phi(\tau') | 0 \rangle = \frac{1}{(2\pi)^{d-1}} \int \frac{d^{d-1}k}{2\omega} e^{-i\omega(t-t'-i\epsilon(t+i')) + i\mathbf{k} \cdot (\mathbf{x}-\mathbf{x}'-i\epsilon(\dot{\mathbf{x}}+\dot{\mathbf{x}}'))} . \quad (14)$$

The regularization introduced by the smearing of the field in the detector's rest frame may be viewed as an ultraviolet cut-off where high frequencies as seen by the detector are cut-off (as opposed to the high frequencies as seen by an inertial observer which are cut-off by the usual  $i\epsilon$ -prescription). The frequency is the time component of the 4-momentum. Given that the 4-momentum in the usual Minkowski frame is  $(\omega, \mathbf{k})^\top$  we find via a straightforward calculation that the time component of this 4-vector in the Fermi frame at time  $\tau$  is  $\omega t(\tau) - \mathbf{k} \cdot \dot{\mathbf{x}}(\tau)$ . The regularization in (14) is seen to be equivalent to an exponential cut-off of the high frequency modes, as seen in the detector's frame, at times  $\tau$  and  $\tau'$ .

The integrals in (14) may also be done by transforming to hyperspherical coordinates. The result is

$$\begin{aligned} \langle 0 | \phi(\tau) \phi(\tau') | 0 \rangle &= \frac{\Gamma[d/2-1]}{4\pi^{d/2}} \frac{1}{A^{d/2-1}} , \\ A &= [i^2(t(\tau) - t(\tau') - i\epsilon(\dot{t}(\tau) + \dot{t}(\tau')))^2 + (\mathbf{x}(\tau) - \mathbf{x}(\tau') - i\epsilon(\dot{\mathbf{x}}(\tau) + \dot{\mathbf{x}}(\tau')))^2] . \end{aligned} \quad (15)$$

We note here that following a similar calculation to that given above the usual  $i\epsilon$  regularization of the correlation function may also be obtained by considering a spatially smeared field. The difference from the above regularization is that the smearing is done in the Minkowski reference frame, that is, always with respect to inertial observers, and not in the Fermi frame. This model detector is thus not rigid in its rest frame.

First we consider the transition rate (7) with the correlation function (15) for a detector following an inertial trajectory. Consider therefore the trajectory  $t = \tau$ ,  $\mathbf{x} = \text{constant}$ , where  $-\infty < \tau < \infty$ . If the detector is switched on in the infinite past,  $\tau_0 = -\infty$ , the transition rate is

$$\dot{F}_\tau(\omega) = \frac{\Gamma[d/2 - 1]}{4\pi^{d/2}} \int_{-\infty}^{\infty} ds \frac{e^{-i\omega s}}{[i^2(s - 2i\epsilon)^2]^{d/2-1}}. \quad (16)$$

Note that we obtain the same expression in this case if we use instead the usual correlation function i.e. with the  $i\epsilon$  regularization. The integral may be done by residues and the result as  $\epsilon \rightarrow 0$  is

$$\dot{F}_\tau(\omega) = \frac{\Gamma[d/2 - 1](-\omega)^{d-3}}{2\pi^{d/2-1}(d-3)!} \Theta(-\omega), \quad (17)$$

where  $\Theta(-\omega)$  is the Heaviside step function. As expected the transition rate vanishes for  $\omega > 0$ , indicating that an inertial detector is not excited by the Minkowski vacuum. For  $\omega < 0$  the transition rate is non-zero due to the possibility of spontaneous emission by the detector.

Next consider the transition rate for a spatially extended detector whose centre follows the uniformly accelerated worldline (9). The transition rate is

$$\dot{F}_\tau(\omega) = \frac{\Gamma[d/2 - 1]}{i^{d-2}(4\pi)^{d/2}} \int_{-\Delta\tau}^{\Delta\tau} ds \frac{e^{-i\omega s}}{(\alpha \sinh(\frac{s}{2\alpha}) - i\epsilon \cosh(\frac{s}{2\alpha}))^{d-2}}. \quad (18)$$

In the case of a detector switched on in the infinite past,  $\tau_0 = -\infty$ , the integral here may be done by residues. The transition rate is independent of  $\tau$  along the trajectory and is given by

$$\begin{aligned} \dot{F}_\tau(\omega) = & \frac{\pi}{2^{d-2}\pi^{(d-1)/2}\alpha^{d-3}\Gamma((d-1)/2)} \\ & \times \begin{cases} \frac{\alpha\omega}{(e^{2\pi\omega\alpha}-1)} \prod_{k=1}^{(d-4)/2} \left( \left( \frac{d-2}{2} - k \right)^2 + \alpha^2\omega^2 \right) & d \text{ even} \\ \frac{1}{(e^{2\pi\omega\alpha}+1)} \prod_{k=1}^{(d-3)/2} \left( \left( \frac{d-2}{2} - k \right)^2 + \alpha^2\omega^2 \right) & d \text{ odd} \end{cases}, \end{aligned} \quad (19)$$

where for  $d = 3$  and  $d = 4$  the products  $\prod_{k=1}^{(d-3)/2} \left( \left( \frac{d-2}{2} - k \right)^2 + \alpha^2\omega^2 \right)$  and  $\prod_{k=1}^{(d-4)/2} \left( \left( \frac{d-2}{2} - k \right)^2 + \alpha^2\omega^2 \right)$  in (19) are both 1. The transition rate (19) is as in the literature [29]. It is thermal with characteristic temperature  $T = 1/(2\pi\alpha)$  in the sense that it satisfies the KMS condition

$$\dot{F}_\tau(\omega) = e^{-\omega/T} \dot{F}_\tau(-\omega), \quad (20)$$

at that temperature (see e.g [6]). Further (19) contains the expected “apparent” statistics inversion as we go from odd to even dimensions.

### 3 Massive scalar field

In this section we compute the correlation function for the smeared field operator (10) for a massive scalar field.

The detector model is as in section 2. The field is expanded in modes as in (1) but now with  $\omega = (\mathbf{k}^2 + m^2)^{1/2}$ , where  $m$  is the field mass. The transition rate for the detector is given by (7), where  $\phi(\tau)$  is the smeared field operator (10). The correlation function is given by the expression (13) and following an identical calculation to that which leads to (14) we find

$$\langle 0 | \phi(\tau) \phi(\tau') | 0 \rangle = \frac{1}{(2\pi)^{d-1}} \int \frac{d^{d-1}k}{2\omega} e^{-i\omega(t-t'-i\epsilon(\dot{t}+\dot{t}')) + i\mathbf{k}\cdot(\mathbf{x}-\mathbf{x}'-i\epsilon(\dot{\mathbf{x}}+\dot{\mathbf{x}}'))} , \quad (21)$$

with  $\omega = (\mathbf{k}^2 + m^2)^{1/2}$ .

The integrals here may again be done by moving to hyperspherical coordinates in  $k$ -space. We restrict ourselves now to the case  $d = 4$  (although the arbitrary  $d$  case follows similarly). After performing the angular integrals, we find

$$\langle 0 | \phi(\tau) \phi(\tau') | 0 \rangle = \frac{1}{(2\pi)^2 R} \int_0^\infty dk \frac{k}{(k^2 + m^2)^{1/2}} \sin(kR) e^{-i(k^2 + m^2)^{1/2}(t-t'-i\epsilon(\dot{t}+\dot{t}'))} , \quad (22)$$

where  $R = \sqrt{(\mathbf{x} - \mathbf{x}' - i\epsilon(\dot{\mathbf{x}} + \dot{\mathbf{x}}'))^2}$ . This may be written as

$$\langle 0 | \phi(\tau) \phi(\tau') | 0 \rangle = \frac{-1}{8\pi^2 R} \partial_R \int_{-\infty}^\infty dk \frac{1}{(k^2 + m^2)^{1/2}} e^{-i((k^2 + m^2)^{1/2}(t-t'-i\epsilon(\dot{t}+\dot{t}')) - kR)} . \quad (23)$$

We now change variables by  $k = m \sinh \theta$ , so that  $\omega = m \cosh \theta$  and

$$\langle 0 | \phi(\tau) \phi(\tau') | 0 \rangle = \frac{-1}{8\pi^2 R} \partial_R \int_{-\infty}^\infty d\theta e^{im(R \sinh \theta - (t-t'-i\epsilon(\dot{t}+\dot{t}')) \cosh \theta)} . \quad (24)$$

For the detector trajectory we consider only timelike worldlines,  $(t - t') > (\mathbf{x} - \mathbf{x}')$ . We distinguish two cases. Firstly, for  $(t - t') > 0$ , we make the substitution  $(t - t' - i\epsilon(\dot{t} + \dot{t}')) = \sqrt{\lambda} \cosh \theta_0$ ,  $R = \sqrt{\lambda} \sinh \theta_0$ , with  $\lambda = (t - t' - i\epsilon(\dot{t} + \dot{t}'))^2 - R^2$ . We find

$$\langle 0 | \phi(\tau) \phi(\tau') | 0 \rangle = \frac{-1}{8\pi^2 R} \partial_R \int_{-\infty}^\infty d\theta e^{-im\sqrt{\lambda} \cosh(\theta_0 - \theta)} . \quad (25)$$

Now we note

$$K_0(z) = \frac{1}{2} \int_{-\infty}^\infty dt e^{-z \cosh t} , \quad (26)$$

valid for  $Re(z) > 0$  [30], where  $K_0$  is a modified Bessel function, and we may show for a timelike worldline that  $Im(\sqrt{\lambda}) < 0$ . Hence

$$\begin{aligned} \langle 0 | \phi(\tau) \phi(\tau') | 0 \rangle &= \frac{-1}{4\pi^2 R} \partial_R \left[ K_0 \left( im\sqrt{\lambda} \right) \right] \\ &= -\frac{im}{4\pi^2 \sqrt{\lambda}} K_1 \left( im\sqrt{\lambda} \right) , \end{aligned} \quad (27)$$

as  $\partial_z K_0(z) = K_1(z)$ . The case  $(t - t') < 0$  is similar except we make the change of variables  $(t - t' - i\epsilon(\dot{t} + \dot{t}')) = -\sqrt{\lambda} \cosh \theta_0$ ,  $R = \sqrt{\lambda} \sinh \theta_0$  again we may use the integral representation of  $K_0$  and we obtain the same result (27).

The massless limit is easily checked. We have near  $z = 0$ ,  $K_1(z) = 1/z$  [30] and so the correlation function (27) agrees with that of Schlicht [1] in this limit. Had we used the field operator without smearing we would have obtained (23) with  $\epsilon = 0$ . The usual regularization procedure, as with the massless case, would then be to introduce a cut-off in the high frequency modes by  $t \rightarrow t - i\eta$ , where  $\eta$  is small. The result would be (27) but with  $\lambda = (t - t' - i\eta)^2 - |\mathbf{x} - \mathbf{x}'|^2$ .

## 4 Detector on Quotient spaces

In this section we adapt the detector model of section 2 to spacetimes built as quotients  $M/\Gamma$  of Minkowski space under certain discrete symmetry groups  $\Gamma$ . In particular we calculate responses on  $M_0$ ,  $M_-$  [9, 10, 31], Minkowski space with an infinite plane boundary and certain conical spacetimes.

As these quotient spaces do not have infinite spatial sections in all directions, it does not directly make sense to consider a detector with infinite spatial extent as used in (10). We shall argue however that we may introduce a detector similar to that of section 2 by working with automorphic fields on  $M$  [7, 8].

Consider Minkowski space  $M$  in  $d$  dimensions, and consider the quotient space  $M/\Gamma$  where  $\Gamma$  is some discrete isometry group.  $|\Gamma|$  may be infinite (as indeed is the case on  $M_0$  and  $M_-$ ) which will mean that some of the following expressions remain formal in those cases. We will find however that these formalities do not interfere as in any calculations done the infinities and the formally vanishing normalization factors will cancel to give finite results.

The automorphic field  $\hat{\phi}$  is constructed from the ordinary field  $\phi$  as the sum

$$\hat{\phi}(x) := \frac{1}{\left(\sum_{\gamma \in \Gamma} p(\gamma)^2\right)^{1/2}} \sum_{\gamma \in \Gamma} p(\gamma) \phi(\gamma^{-1}x) , \quad (28)$$

where  $p(\gamma)$  is a representation of  $\Gamma$  in  $SL(\mathbb{R}) \simeq \{1, -1\}$ . The normalization in (28) has been chosen so that, at equal times

$$[\hat{\phi}(x), \dot{\hat{\phi}}(x')] = i\delta^{(d-1)}(x - x') + \text{image terms} . \quad (29)$$

The two point function for the automorphic field is then given by the method of images as

$$\langle 0 | \hat{\phi}(x) \hat{\phi}(x') | 0 \rangle = \sum_{\gamma \in \Gamma} p(\gamma) \langle 0 | \phi(x) \phi(\gamma^{-1}x') | 0 \rangle , \quad (30)$$

where  $\langle 0 | \phi(x) \phi(x') | 0 \rangle$  is the usual correlation function on Minkowski space.

As a model of a particle detector on  $M/\Gamma$ , we introduce on  $M$  a detector linearly coupled to the automorphic field by

$$H_{\text{int}} = cm(\tau) \hat{\phi}(\tau) , \quad (31)$$

with<sup>2</sup>

$$\hat{\phi}(\tau) = \int d^{d-1} \xi W_\epsilon(\xi) \hat{\phi}(x(\tau, \xi)) . \quad (32)$$

---

<sup>2</sup>If we considered here  $\hat{\phi}(\tau) = \hat{\phi}(x(\tau))$  with the usual  $i\epsilon$  regularization, again we would find as Schlicht does in Minkowski space an unphysical result for the response of the uniformly accelerated detector on these spacetimes. This is most easily seen by considering that the  $\gamma = I$  term (where  $I$  is the identity element) in (30) is that found in Minkowski space.

One might ask why we have not included in (31) image terms under  $\Gamma$  (that is one term for each image of the detector). There are two obvious ways in which such terms could be included. Firstly we could consider each image term in the sum to be weighted by the representation  $p(\gamma)$ . In certain situations, such as on Minkowski space with an infinite plane boundary with Dirichlet boundary conditions this would however lead to the detector and its image terms cancelling each other to give a vanishing interaction Hamiltonian. Alternatively we could consider image terms without the representation weights. Then each image term would be equal to that in (31) and so we would obtain the same results with an overall (possibly infinite) normalisation factor, which can be absorbed in the coefficient  $c$ . We therefore work with (31).

From (31), a discussion analogous to that in section 2 leads to the transition rate (to first order in perturbation theory)

$$\dot{F}_\tau(\omega) = 2 \int_0^\infty ds \operatorname{Re} \left( e^{-i\omega s} \langle 0 | \hat{\phi}(\tau) \hat{\phi}(\tau-s) | 0 \rangle \right) , \quad (33)$$

where the correlation function for the automorphic field in (33),  $\langle 0 | \hat{\phi}(\tau) \hat{\phi}(\tau-s) | 0 \rangle$ , is given by the method of images applied to (15).

## 4.1 $M_0$

$M_0$  is a quotient of 4-dimensional Minkowski space where the quotienting group  $\Gamma$  is that generated by the isometry  $J_0 : (t, x, y, z) \mapsto (t, x, y, z + 2a)$ . The transition rate for our detector is given by (33) with

$$\langle 0 | \hat{\phi}(\tau) \hat{\phi}(\tau') | 0 \rangle = \sum_{n \in \mathbb{Z}} \eta^n \langle 0 | \phi(\tau) \phi(J_0^n \tau') | 0 \rangle , \quad (34)$$

where  $\eta = +1, (-1)$  are the representations of  $\Gamma$ , labelling untwisted (twisted) fields respectively.

### 4.1.1 Inertial detector on $M_0$

Consider first a detector following the inertial trajectory

$$\begin{aligned} t &= \tau(1-v^2)^{-1/2} , & z &= \tau v(1-v^2)^{-1/2} , \\ x &= x_0 , & y &= y_0 , \end{aligned} \quad (35)$$

where velocity  $-1 < v < 0$ ,  $-\infty < \tau < \infty$  is the detector's proper time and  $x_0, y_0$  are constants. Substituting the trajectory into (34) and then (33), we find that the transition rate for a detector switched on in the infinite past reads

$$\dot{F}_\tau(\omega) = -\frac{1}{4\pi^2} \sum_{n=-\infty}^{\infty} \eta^n \int_{-\infty}^{\infty} ds \frac{e^{-i\omega s}}{(s-2i\epsilon)^2 + 4nav(s-2i\epsilon)(1-v^2)^{-1/2} - (2na)^2} . \quad (36)$$

The integral may be done by residues. The result is

$$\dot{F}_\tau(\omega) = -\frac{(1-v^2)^{1/2}}{4\pi a} \sum_{n=-\infty}^{\infty} \eta^n \frac{\sin(2\omega na(1-v^2)^{-1/2})}{n} e^{\frac{2\omega nav}{(1-v^2)^{1/2}}} \Theta(-\omega) . \quad (37)$$

As on Minkowski space the transition rate vanishes for  $\omega > 0$  while it is non-zero for  $\omega < 0$  although the rate of spontaneous emission is altered from the Minkowski rate due to the non-trivial topology. The transition rate depends on velocity  $v$  due to the absence of a boost Killing vector in the  $z$  direction on  $M_0$ .

Consider now the limit as  $v \rightarrow 0$ . By the isometries of  $M_0$  this gives the response of an inertial detector that may have arbitrary velocity in the  $x$  or  $y$  directions. Then

$$\dot{F}_\tau(\omega) = \left( -\frac{\omega}{2\pi} + \frac{1}{2\pi a} \sum_{n=1}^{\infty} \eta^n \frac{1}{n} \sin(-2n\omega a) \right) \Theta(-\omega) . \quad (38)$$

In the case of an untwisted field,  $\eta = 1$ , the summation in (38) is recognized as the Fourier series of the  $2\pi$ -periodic function that on the interval  $(0, 2\pi)$  takes the form  $f(-2\omega a) = \frac{1}{2}(\pi + 2\omega a)$  (see e.g. [32]). We hence find

$$\dot{F}_\tau(\omega) = \frac{\left(\left[\frac{-\omega a}{\pi}\right] + \frac{1}{2}\right)}{2a} \Theta(-\omega) , \quad (39)$$

where  $[x]$  denotes the integer part of  $x$ .

For a twisted field,  $\eta = -1$ , we note  $(-1)^n \sin(nx) = \sin(n(x + \pi))$  and find

$$\dot{F}_\tau(\omega) = \frac{\left[\frac{-\omega a}{\pi} + \frac{1}{2}\right]}{2a} \Theta(-\omega) . \quad (40)$$

#### 4.1.2 Uniformly accelerated detector

If we consider a detector following the worldline of uniform acceleration (9) we obtain, again for the detector switched on at  $\tau_0 = -\infty$ ,

$$\dot{F}_\tau(\omega) = \frac{\omega}{2\pi(e^{2\pi\alpha\omega} - 1)} \left( 1 + \sum_{n=1}^{\infty} \eta^n \frac{\sin[2\alpha\omega \operatorname{arc sinh}(na/\alpha)]}{na\omega\sqrt{1+n^2a^2/\alpha^2}} \right) , \quad (41)$$

where the integral in the transition rate has again been done by residues. The result agrees with that obtained by Louko and Marolf in [9]. The response is independent of  $\tau$ . Moreover it is thermal in the sense that it satisfies the KMS condition (20). There is however a break from the purely Planckian form found on Minkowski space.

## 4.2 Minkowski space with an infinite plane boundary

In this subsection we consider a detector on  $d$ -dimensional Minkowski space,  $d > 2$ , with Minkowski coordinates  $(t, x_1, \dots, x_{d-1})$ , with an infinite boundary at  $x_1 = 0$ . Detectors on this spacetime (in particular in the case of 4-dimensions) have been considered by a number of authors (see e.g. [33, 34])<sup>3</sup>. However there has not been any presentations (as far as the author is aware) of the time dependent response for an inertial or uniformly accelerated observer who approaches the boundary from

---

<sup>3</sup>The case of Dirichlet boundary conditions for  $d = 4$  has been the focus of some study recently on the response of detectors to negative energy [12]. The authors of [12] considered the response of a finite time detector travelling inertially parallel to the boundary. They found that the negative energy outside the boundary has the effect of decreasing the excitations which are present even in Minkowski space due to the switching of the detector.

infinity. The results in this section are interesting also as a preliminary calculation before the response of detectors on  $M_-$  is considered. Many of the features seen here will also be observed there, but in a simpler context as there is no compact direction and therefore the image sum is finite. Further we will see in section 7.2 that the response of a uniformly accelerated detector on four-dimensional Minkowski space with an infinite plane boundary is very closely related to the response of an inertial detector coupled to a conformal scalar field in  $\mathbb{R}P^3$  de Sitter space [11].

Again the discussion of section 4 follows through and the transition rate is given by (33) where now the automorphic correlation function is

$$\langle 0 | \hat{\phi}(\tau) \hat{\phi}(\tau') | 0 \rangle = \sum_{n=0,1} \beta^n \langle 0 | \phi(\tau) \phi(J_b^n \tau') | 0 \rangle , \quad (42)$$

where  $J_b : (t, x_1, x_2, \dots, x_{d-1}) \mapsto (t, -x_1, x_2, \dots, x_{d-1})$  and  $\beta = +1, (-1)$ , which label Neumann and (Dirichlet) boundary conditions respectively. We note here that on four-dimensional Minkowski space with boundary at  $x = 0$  the renormalized expectation values  $\langle 0 | T_{\mu\nu} | 0 \rangle$  of the energy-momentum tensor for the minimally coupled massless scalar field in the vacuum state induced by the Minkowski vacuum are [2, 31]

$$\langle 0 | T_{tt} | 0 \rangle = -\langle 0 | T_{yy} | 0 \rangle = -\langle 0 | T_{zz} | 0 \rangle = \beta \frac{1}{16\pi^2 x^4} , \quad \langle 0 | T_{xx} | 0 \rangle = 0 . \quad (43)$$

#### 4.2.1 Inertial detector

Firstly we consider an inertial detector with motion parallel to the boundary. Due to the isometries of the spacetime we may consider, without loss of generality, the trajectory  $t = \tau$ ,  $x_1 = \lambda$ ,  $x_i = 0$  for  $1 < i \leq d-1$  where  $\lambda$ , the distance from the boundary, is constant. The transition rate contains two terms. The first one comes from the first term in the boundary space correlation function (42) and equals the corresponding transition rate on Minkowski space. For a detector switched on in the infinite past this is given by (17). The second term, comes from the image term in (42), and is given by

$$\dot{F}_{B\tau}(\omega) = \frac{\beta \Gamma(d/2 - 1)}{4\pi^{d/2}} \int_{-\infty}^{\infty} ds \frac{e^{-i\omega s}}{[i^2(s - 2i\epsilon)^2 + (2\lambda)^2]^{d/2-1}} . \quad (44)$$

The integral in (44) can be evaluated by residues. Specialising to 4 dimensions, the total transition rate including the Minkowski part is found to be

$$\dot{F}_{\tau}(\omega) = \left( -\frac{\omega}{2\pi} - \frac{\beta}{4\pi\lambda} \sin(2\omega\lambda) \right) \Theta(-\omega) . \quad (45)$$

In figure 1 we plot  $\dot{F}_{\tau}(\omega)/|\omega|$  against  $|\omega|\lambda$  for Neumann boundary conditions. On the boundary the rate is twice that in Minkowski space, while far from the boundary the rate becomes that on Minkowski space. For Dirichlet boundary conditions the transition rate vanishes on the boundary as expected. Our results agree with those in [33].

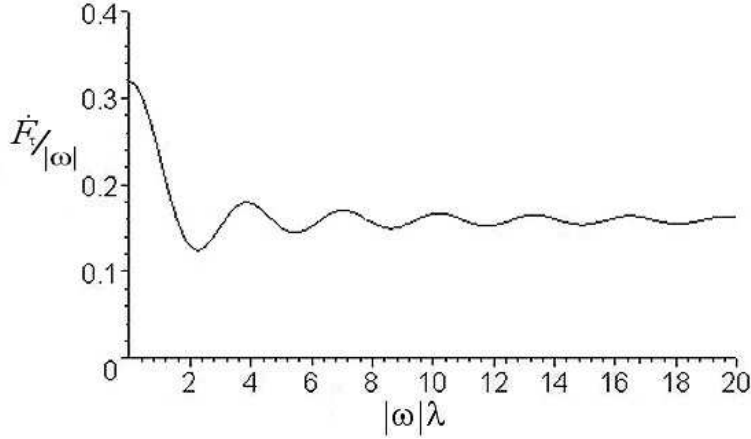


Figure 1: Transition rate for inertial detector moving parallel to the boundary, as a function of distance  $\lambda$  from the boundary. We have taken  $\omega < 0$  and plotted  $\dot{F}_\tau(\omega)/|\omega|$  against  $|\omega|\lambda$  for Neumann boundary conditions.

Next, restricting ourselves to  $d = 4$  again, we consider an inertial detector approaching the boundary from infinity following the worldline

$$\begin{aligned} t &= \tau(1-v^2)^{-1/2}, & x &= \tau v(1-v^2)^{-1/2}, \\ y &= y_0, & z &= z_0, \end{aligned} \quad (46)$$

with  $-1 < v < 0$  and  $-\infty < \tau < 0$ . We expect the response in this case to be dependent on proper time  $\tau$ , as the boundary breaks the translation invariance of Minkowski space in the  $x$ -direction.

Again the transition rate is in two parts. The Minkowski part (the  $n = 0$  term) will lead again to the Minkowski space rate (17). For a detector switched on the the infinite past this part reads

$$\dot{F}_{M\tau}(\omega) = -\frac{\omega}{2\pi} \Theta(-\omega), \quad (47)$$

where  $\Theta(-\omega)$  is a step function, and  $M$  denotes that this is the Minkowski term. The Minkowski term of course is independent of  $\tau$ . It is the image term in the correlation function which leads to a  $\tau$ -dependent result. The image part of the transition rate is

$$\dot{F}_{B\tau}(\omega) = -\frac{\beta}{2\pi^2} (1-v^2) \lim_{\epsilon \rightarrow 0} \int_0^\infty ds \operatorname{Re} \left( \frac{e^{-i\omega s}}{(s-2i\epsilon)^2 - v^2(s-2\tau)^2} \right). \quad (48)$$

The integral may be evaluated, using some contour arguments, in terms of sine and cosine integrals. We find

$$\begin{aligned} \dot{F}_\tau(\omega) &= -\frac{\beta}{2\pi^2(b+c)} (-\operatorname{Ci}(b|\omega|) \cos(b|\omega|) - \operatorname{si}(b|\omega|) \sin(b|\omega|) \\ &\quad + \operatorname{Ci}(c|\omega|) \cos(c|\omega|) + \operatorname{si}(c|\omega|) \sin(c|\omega|) + 2\pi \sin(b\omega) \Theta(-\omega)), \end{aligned} \quad (49)$$

where  $\operatorname{Ci}$ ,  $\operatorname{si}$  are the cosine and shifted sine integrals [35],  $b = 2v\tau/(1+v)$  and  $c = 2v\tau/(1-v)$ .

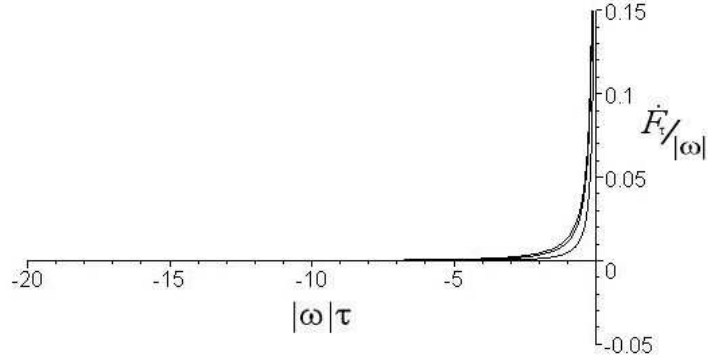


Figure 2: Transition rate for inertial detector approaching boundary with Neumann boundary conditions and  $\omega > 0$ .  $\dot{F}_\tau(\omega)/|\omega|$  is plotted against  $|\omega|\tau$  for  $v = -1/2$  (lower curve near the axis),  $v = -1/3$  and  $v = -1/4$  (upper curve).

In figure 2 we plot  $\dot{F}_\tau(\omega)/|\omega|$  against  $|\omega|\tau$  for  $\omega > 0$ , Neumann boundary conditions and for various values of  $v$ . We note that for  $\omega > 0$  the transition rate is non-zero, in contrast to the response of an inertial detector travelling parallel to the boundary, and diverges as the boundary is reached.

For  $\omega < 0$  recall that the Minkowski part of the transition rate is non zero. We plot the total rate for  $\omega < 0$  in figure 3. In both cases the response depends on the

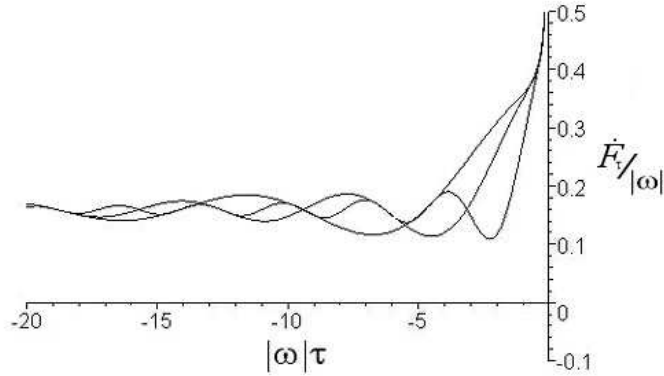


Figure 3: Transition rate for inertial detector approaching boundary with Neumann boundary conditions and  $\omega < 0$ .  $\dot{F}_\tau(\omega)/|\omega|$  is plotted against  $|\omega|\tau$  for  $v = -1/2$  (lower curve),  $v = -1/3$  and  $v = -1/4$  (upper curve).

velocity, as expected since there is no boost isometry in the  $x$ -direction. Further in both cases we may show that the divergence at  $x = 0$  goes as  $1/\tau$  and so is weaker than that in the energy expectation values (43). It can also be verified that the transition rate dies off at  $\tau = -\infty$  as  $O(1/\tau^3)$ . Further numerical evidence suggests that the divergences persist for a detector that is switched on at a finite time.

### 4.2.2 Uniformly accelerated detectors

Consider now a uniformly accelerated detector with acceleration parallel to the boundary and switched on in the infinite past. We may consider without loss of generality the worldline

$$\begin{aligned} t &= \alpha \sinh(\tau/\alpha) , \\ x_1 &= \lambda , \\ x_2 &= \alpha \cosh(\tau/\alpha) , \\ x_i &= 0 , \quad 2 < i \leq d-1 . \end{aligned} \quad (50)$$

The response again is in two parts. The first term in (42) leads to the thermal transition rate an accelerated detector on Minkowski space (19). The image part of the correlation function on the worldline (50) is

$$\langle 0 | \phi(\tau) \phi(J_B \tau') | 0 \rangle = \frac{\beta \Gamma[d/2 - 1]}{i^{d-2} 4\pi^{d/2}} \frac{1}{\left( 4 \left( \alpha \sinh\left(\frac{\tau-\tau'}{2\alpha}\right) - i\epsilon \cosh\left(\frac{\tau-\tau'}{2\alpha}\right) \right)^2 - (2\lambda)^2 \right)^{d/2-1}} , \quad (51)$$

which as expected is invariant under  $\tau$  translations. Restricting now to 4 dimensions, the boundary part of the transition rate is

$$\dot{F}_{B\tau}(\omega) = -\frac{\beta}{4\pi^2} \int_{-\infty}^{\infty} ds \frac{e^{-i\omega s}}{\left( 4 \left( \alpha \sinh\left(\frac{s}{2\alpha}\right) - i\epsilon \cosh\left(\frac{s}{2\alpha}\right) \right)^2 - (2\lambda)^2 \right)} . \quad (52)$$

The integral can be done by residues. The result is

$$\dot{F}_{B\tau}(\omega) = \frac{\beta}{4\pi} \frac{\alpha}{\lambda(\alpha^2 + \lambda^2)^{1/2}} \frac{1}{(e^{2\pi\omega\alpha} - 1)} \sin(2\omega\alpha \operatorname{arcsinh}(\lambda/\alpha)) , \quad (53)$$

which agrees with [33]. The response is thermal in the sense that it satisfies the KMS condition at temperature  $T = (2\pi\alpha)^{-1}$ .

Now let us consider the uniformly accelerated worldline (9). The acceleration is now perpendicular to the boundary. We begin by considering the detector switched on in the infinite past. The Minkowski part of the correlation function again leads to the thermal response (19). The image term on worldline (9) gives

$$\langle 0 | \phi(\tau) \phi(J_B \tau') | 0 \rangle = \frac{\beta \Gamma[d/2 - 1]}{4\pi^{d/2} \left( (4\alpha^2 + 4\epsilon^2) \cosh^2\left(\frac{\tau+\tau'}{2\alpha}\right) \right)^{d/2-1}} . \quad (54)$$

It may be argued by the dominated convergence theorem that the  $\epsilon$  can be dropped when calculating the transition rate. The geometrical reason is that the worldline and its image under  $J_B$  are totally spacelike separated, and so the correlation function required in the transition rate contains no divergences in the integration region.

The image term of the transition rate is thus

$$\dot{F}_{B\tau}(\omega) = \frac{\beta \Gamma[d/2 - 1]}{2\pi^{d/2}} \int_0^{\infty} ds \frac{\cos(\omega s)}{\left( 2\alpha \cosh\left(\frac{2\tau-s}{2\alpha}\right) \right)^{d-2}} . \quad (55)$$

We see immediately that this part of the transition rate is even in  $\omega$  and hence the boundary term breaks the KMS condition (20). In this sense the response is non-thermal and non-Planckian.

Consider now the 4-dimensional case,  $d = 4$ . When  $\tau = 0$  we can do the integral in (55) analytically, with the result

$$\dot{F}_{B0}(\omega) = \frac{\beta\omega}{4\pi \sinh(\omega\pi\alpha)} . \quad (56)$$

For general  $\tau$  we may compute the integral numerically for different values of  $\alpha$ ,  $\tau$  and  $\omega$ . We have done this with the help of Maple. For  $\alpha = 1$  we find the total transition rate (including the thermal part) displayed in figure 4. Note that for

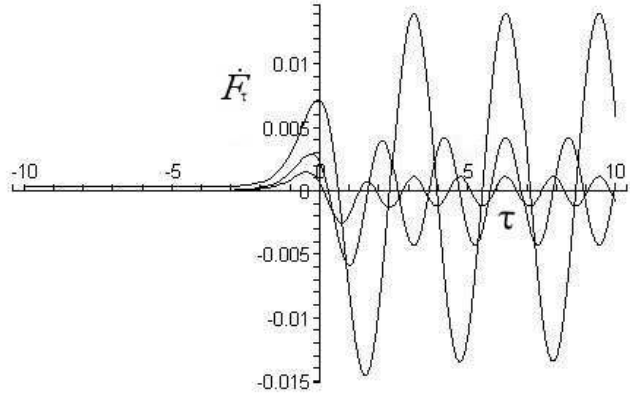


Figure 4: Transition rate for uniformly accelerated detector approaching boundary with Neumann boundary conditions, for  $\alpha = 1$ ,  $\omega = 1$  (upper curve),  $\omega = 1.5$  and  $\omega = 2$  (lower curve).

many switch off times  $\tau$  the image part dominates the Minkowski part. Further we can prove analytically, by changing variables in (55) by  $s = 2\alpha x + 2\tau$  expanding the cos function and evaluating the resulting integrals, that the image part of the transition rate is given by

$$\dot{F}_{B\tau}(\omega) = \frac{\beta\omega \cos(2\tau\omega)}{2\pi \sinh(\omega\pi\alpha)} + B_\tau(\omega) , \quad (57)$$

where the function  $B_\tau(\omega)$  is bounded in absolute value by  $\frac{\beta}{2\pi^2\alpha} e^{-\frac{2\tau}{\alpha}}$ . Therefore for large but finite  $\tau$  the image part of the transition rate is found not to tend to 0 but instead is periodic in  $\tau$  with period  $\pi/\omega$ .<sup>4</sup> This is a property only of the transition rate of a detector which is turned on in the infinite past.

Considering now a detector switched on at finite time  $\tau_0$  (which recall is the more realistic situation). The image part of the transition rate is given by (55) with the upper limit of the integral replaced by  $\tau - \tau_0$ . In figure 5 we plot this image part of the transition rate only, when the switching of the detector is instantaneous

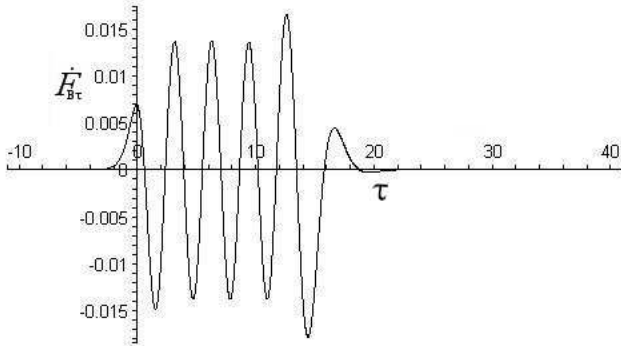


Figure 5: Image term of the transition rate of a uniformly accelerated detector approaching the boundary with Neumann boundary conditions for a detector switched on at  $\tau_0 = -15$ , for  $\alpha = 1$ ,  $\omega = 1$ .

for,  $\tau_0 = -15$ ,  $\alpha = 1$  and  $\omega = 1$ . We find that when the detector is switched on only for a finite time the transition rate is periodic for some time however falls off to the usual thermal response at late  $\tau$ . We have proven this via an analytic calculation, by changing variables in (55) (with upper limit  $\tau - \tau_0$ ) by  $s = -2\alpha y + 2\tau$  expanding the  $\cos$  function and showing the resulting integrals are bounded in absolute value by  $Ae^{-B\tau}$  where  $A$  and  $B$  are positive constants.

In the case of instantaneous switching it was found that even for the inertial detector in Minkowski space the response function for a finite time detection includes a logarithmic divergence [36]. The transition rate however, although altered from the infinite time case, is finite for all non-zero finite time detections. Further in [37] it was shown that the divergence in the response rate is due to the instantaneous switching: if the detector is switched on smoothly, no divergence occurs. It is interesting then to briefly investigate the effect of smooth switching on the results obtained above. We introduce therefore a smooth window function in time  $\tau$  into the transition rate (7), that is we consider the rate

$$\dot{F}_{\tau, \tau_0}(\omega) = 2 \int_0^\infty ds W(s, \tau - \tau_0) \operatorname{Re} (e^{-i\omega s} \langle 0 | \phi(\tau) \phi(\tau - s) | 0 \rangle) , \quad (58)$$

where  $W(s, \tau - \tau_0)$  is a smooth window function with characteristic length  $\tau - \tau_0$ . In particular we consider exponential and Gaussian switching functions

$$W_1(s, \tau - \tau_0) = e^{-\frac{|s|}{\tau - \tau_0}} , \quad (59)$$

$$W_2(s, \tau - \tau_0) = e^{-\frac{s^2}{2(\tau - \tau_0)^2}} . \quad (60)$$

The effect of these window functions on the response of a uniformly accelerated detector in Minkowski space was investigated in [38]. Here we will only consider the effect on the image part of the transition rate on Minkowski space with boundary.

<sup>4</sup>For arbitrary dimension we may prove that the image part of the transition rate consists of a term periodic in  $\tau$  with period  $\pi/\omega$  plus a term bounded in absolute value by  $(\text{constant})e^{-\frac{(d-2)\tau}{2\alpha}}$ .

Substituting the image term (54) and one of the window functions (59), (60) into the transition rate (58), we may calculate the integral numerically. In figures 6 and 7 we plot the transition rate in four-dimensions for a sample of the parameters and with exponential and Gaussian switching respectively. The numerical results

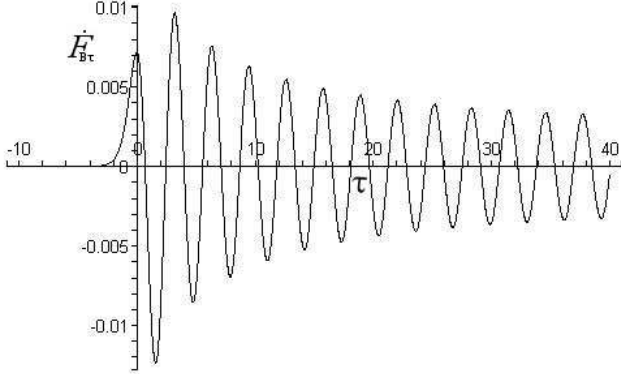


Figure 6: Image term of the transition rate of a uniformly accelerated detector approaching boundary with Neumann boundary conditions for a detector switched on at  $\tau_0 = -15$  with an exponential switching function, for  $\alpha = 1, \omega = 1$ .

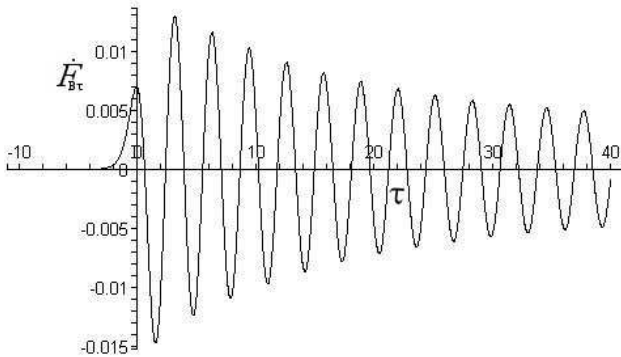


Figure 7: Image term of the transition rate of a uniformly accelerated detector approaching boundary with Neumann boundary conditions for a detector switched on at  $\tau_0 = -15$  with a Gaussian switching function, for  $\alpha = 1, \omega = 1$ .

suggest that in all cases of finite time detection the image part of the transition rate tends to 0 as the detection time tends to infinity. That is, the transition rate tends to that on Minkowski space in this limit, as expected as in this limit the detector recedes infinitely far from the boundary. It is an interesting result that this was not the case for a detector switched on in the infinite past. This suggests that in this case the  $\tau_0 \rightarrow -\infty$  limit should be taken after the transition rate integral has been done.

### 4.3 Conical singularity and generalisations

In this section we consider the response of a uniformly accelerated detector following trajectory (9) on the quotient space of Minkowski space under the group generated by the involution  $J_{c_2} : (t, x, y, z) \mapsto (t, -x, -y, z)$ . Further we consider the higher dimensional generalisation of this spacetime constructed as the quotient of  $d$ -dimensional Minkowski space under the involution  $J_{c_k} : (t, x_1, x_2, \dots, x_{d-1}) \mapsto (t, -x_1, -x_2, \dots, -x_k, x_{k+1}, \dots, x_{d-1})$  where  $1 < k < d$ . For reasons discussed later the response on these higher dimensional spaces will be relevant when we consider the response of static detectors on the  $\mathbb{RP}^3$  geon in section 6 and inertial detectors on  $\mathbb{RP}^3$  de Sitter space in section 7.

These spacetimes are conifolds [39, 40]. As quotients of Minkowski space under an involution with fixed points they are flat away from these  $(d - k)$ -dimensional hypersurfaces of fixed points but may be considered to have a distributional curvature on them (see e.g [41, 42]). The spacetime  $M/J_{c_2}$  is sometimes referred to as a conical spacetime as it has a conical singularity at  $x_1 = x_2 = 0$ . Transforming to cylindrical coordinates by  $x_1 = r \cos \phi$ ,  $x_2 = r \sin \phi$ , the isometry takes the form  $J_{c_2} : (t, r, \phi, x_3, \dots, x_{d-1}) \mapsto (t, r, \phi + \pi, x_3, \dots, x_{d-1})$  and the metric reads

$$ds^2 = dt^2 - dr^2 - r^2 d\phi^2 - (dx_3)^2 - \dots - (dx_{d-1})^2, \quad (61)$$

where  $dr^2 + r^2 d\phi^2$  with the identification  $(r, \phi) \sim (r, \phi + \pi)$  is the metric on a cone with deficit angle  $\pi$ . In 4 dimensions  $M/J_{c_2}$  may be considered as the spacetime outside an idealized, cosmic string [43] with “gravitational mass per unit length”  $\mu = 1/8$  (see [44]).

First we note that for an inertial or uniformly accelerated detector whose motion is in any direction  $x_i$  with  $k < i < d$ , the response on these spacetimes will be the same as that of a detector at rest or accelerating parallel to the boundary on Minkowski space with boundary (where  $\lambda$  in (45) and (53) is now given by the shortest distance of the detector to the hypersurface of fixed points  $\lambda = ((x_1)^2 + (x_2)^2 + \dots + (x_k)^2)^{1/2}$ ). This can be clearly seen by directly comparing the correlation functions in both cases.

Consider now a particle detector uniformly accelerated with trajectory (9) in the spacetime  $M/J_{c_k}$ . Again as  $J_{c_k}$  is an involution the correlation function consists of two terms,

$$\langle 0 | \hat{\phi}(\tau) \hat{\phi}(\tau') | 0 \rangle = \langle 0 | \phi(\tau) \phi(\tau') | 0 \rangle + \beta \langle 0 | \phi(\tau) \phi(J_{c_k} \tau') | 0 \rangle, \quad (62)$$

where  $\beta = +1, (-1)$  label the two possibilities for the representations of the group in the automorphic field expansion (28). Consider first a detector switched on at  $\tau_0 = -\infty$ . The first term, when substituted into the transition rate (33) on the worldline (9), leads to the thermal response in Minkowski space (19). The transition rate for the image term is

$$\dot{F}_{I\tau(\omega)} = \frac{\beta \Gamma[d/2 - 1]}{2\pi^{d/2}} \int_0^\infty ds \frac{\cos(\omega s)}{\left(4\alpha^2 \cosh^2\left(\frac{2\tau-s}{2\alpha}\right) + C_k\right)^{d/2-1}}, \quad (63)$$

where  $C_k = \sum_{m=2}^k (2x_m)^2$ . As the trajectory and its image are totally spacelike separated we have dropped the regularization in the above expression.

(63) is even in  $\omega$  and so the image term breaks the KMS condition and the response is non-thermal and non-Planckian. Further we may prove that (63) consists of a term periodic in  $\tau$  with period  $\pi/\omega$  and a term which decays exponentially as  $\tau \rightarrow \infty$ . The qualitative behaviour is therefore similar to that of the uniformly accelerated detector on  $M$  with boundary, investigated in section 4.2 (compare (63) with (55)). As in section 4.2 it can be shown also here that for a detector switched on at  $\tau_0 > -\infty$  the image part of the transition rate tends to 0 as  $\tau \rightarrow \infty$ .

For a detector that accelerates towards the surface of fixed points of the involution, that is in the direction  $r = ((x_1)^2 + (x_2)^2 + \dots + (x_k)^2)^{1/2}$ , the response is identical to that on Minkowski space with boundary with acceleration perpendicular to the boundary. In sections 6 and 7 we shall plot (63) for some specific values of  $d$  and  $k$  numerically.

We end this section with a comment on more general cosmic string spacetimes. The methods used above could easily be applied to a larger class of idealized cosmic string spacetimes for which the metric is (61), with the identification  $(r, \phi) \sim (r, \phi + \pi/n)$  where  $n \in \mathbb{Z}$  (and thus a deficit angle of  $\pi(2 - 1/n)$ ), as in these cases the correlation function may be given by a mode sum. Detectors with motion parallel to such cosmic strings have been considered by [22,23]. Their main conclusions, which agree with ours here where they overlap, are that the detector does respond to the presence of the string in a manner which depends on its distance from the string. Our results above and in the previous subsection add to the discussion, as we have been able to show the behaviour of detectors when motion is perpendicular to the string for the specific case of  $n = 1$ . Numerical evaluations of the transition rate for any  $n$  could be done in a similar way, but we shall not pursue this further here. It is important to note however this class of cosmic strings does not include realistic cosmic strings of the GUT scale where the deficit angle is  $\approx 10^{-5}$ .

#### 4.4 Scalar detector on $M_-$

Finally let us consider  $M_-$  [9,10,31] which is a quotient of Minkowski space (or of  $M_0$ , it being a double cover of  $M_-$ ) under the map  $J_- : (t, x, y, z) \mapsto (t, -x, -y, z + a)$ . Our interest in  $M_-$ , as well as it being an interesting topologically non-trivial spacetime in which we can probe the effect of topology on the Unruh effect, lies in its role in modelling, via accelerated observers on flat spacetimes, the Hawking(-Unruh) effect on the  $\mathbb{RP}^3$  geon [9].

Again we may use the method of images to find the correlation function for the automorphic field, with the result

$$\langle 0 | \hat{\phi}(\tau) \hat{\phi}(\tau') | 0 \rangle = \sum_{n \in \mathbb{Z}} \langle 0 | \phi(\tau) \phi(J_- \tau') | 0 \rangle . \quad (64)$$

The transition rate is given by (33).

##### 4.4.1 Inertial detector

Considering a detector following the inertial trajectory (46). The transition rate may again be split into two parts. The first comes from the  $M_0$  part in the image sum (the even  $n$  terms in (64)) and will lead to the same response as on  $M_0$  for

untwisted fields (39). The other part (due to odd  $n$  terms in (64)) is similar to the boundary part of such a detector on  $M$  with boundary, giving in the transition rate the contribution

$$\begin{aligned}\dot{F}_{I\tau(\omega)} = & -\frac{1}{2\pi^2}(1-v^2) \sum_{n=-\infty}^{\infty} \frac{1}{C_n + B_n} (-\text{Ci}(B_n|\omega|) \cos(B_n|\omega|) \\ & -\text{si}(B_n|\omega|) \sin(B_n|\omega|) + \text{Ci}(C_n|\omega|) \cos(C_n|\omega|) + \text{si}(C_n|\omega|) \sin(C_n|\omega|) \\ & + 2\pi \sin(B_n\omega) \Theta(-\omega)) ,\end{aligned}\quad (65)$$

where

$$B_n = \frac{-4\tau v^2 + (16\tau^2 v^2 + 4(1-v^2)^2((2y_0)^2 + (2na+a)^2))^{1/2}}{2(1-v^2)} , \quad (66)$$

$$C_n = \frac{+4\tau v^2 + (16\tau^2 v^2 + 4(1-v^2)^2((2y_0)^2 + (2na+a)^2))^{1/2}}{2(1-v^2)} . \quad (67)$$

In contrast to the analogous result on  $M$  with boundary, there is no divergence here at  $x = 0$  as there is no obstruction there and the inertial detector on  $M_-$  carries through  $x = 0$  smoothly. Note that on  $M_-$  the energy-momentum tensor expectation values are finite over the whole spacetime [9, 31], while on  $M$  with boundary they diverge at  $x = 0$ . For  $\omega > 0$  the  $M_0$  part of the transition rate vanishes while the image part is odd in  $\tau$ . Further, numerical evaluations of the sum indicate that it is non-zero. Here therefore we have an example of a spacetime and trajectory with no pathologies at all where the total transition rate is negative for some values of proper time  $\tau$ .

#### 4.4.2 Uniformly accelerated detector

Consider a detector following the uniformly accelerated worldline (9). Again the correlation function is in two parts. The part coming from the  $M_0$  part of the image sum is given by the corresponding response on  $M_0$  ((41) with  $\eta = -1$ ). This part satisfies the KMS condition and so in this sense is thermal. The “image” part is then somewhat similar to the boundary part found in the case of  $M$  with boundary. The transition rate for this term is

$$\dot{F}_{I\tau}(\omega) = \frac{1}{2\pi^2} \sum_{n=-\infty}^{\infty} \int_0^{\infty} ds \frac{\cos(\omega s)}{4\alpha^2 \cosh^2\left(\frac{2\tau-s}{2\alpha}\right) + 4y_0^2 + a^2(2n-1)^2} , \quad (68)$$

where  $y_0$  is the  $y$  coordinate of the detector. As on Minkowski space with boundary this image part of the transition rate is even in  $\omega$  and so breaks the KMS condition. The transition rate is thus non-thermal and non-Planckian. Further we find, by similar techniques to those leading to (57)

$$\dot{F}_{I\tau}(\omega) = \sum_{n=-\infty}^{\infty} \left( \frac{\alpha \cos(2\tau\omega) \sin(\alpha \omega \text{arccosh}(\frac{c_n}{2\alpha^2}))}{\pi(c_n^2 - 4\alpha^4)^{1/2} \sinh(\omega\pi\alpha)} + B_{n,\tau}(\omega) \right) , \quad (69)$$

where  $c_n = 2\alpha^2 + 4y_0^2 + (2na-a)^2$ , and each  $B_{n,\tau}(\omega)$  is bounded by  $1/(2\pi^2\alpha)e^{-2\tau/\alpha}$ . Further we may show that the sum of  $B_{n,\tau}(\omega)$  over  $n$  is bounded by a function which

exponentially decays as  $\tau \rightarrow \infty$ . We see as with the detector on  $M$  with boundary for large  $\tau$  the response becomes periodic in  $\tau$  with period  $\pi/\omega$ .

We may investigate the general case here numerically. An analytic result is easy to find in the case when  $\tau = 0$ , with the result

$$\dot{F}_{I0}(\omega) = \frac{\alpha}{2\pi} \sum_{n=-\infty}^{\infty} \frac{\sin(\alpha \omega \text{arccosh}(\frac{c_n}{2\alpha^2}))}{(c_n^2 - 4\alpha^4)^{1/2} \sinh(\omega \pi \alpha)}. \quad (70)$$

For a detector switched on instantaneously at a finite time  $\tau_0 > -\infty$  an analytic calculation shows that the difference between the response on  $M_-$  and that on  $M_0$  dies off as  $\tau \rightarrow \infty$ , as would be expected far away from  $x = 0$ . It is an interesting point that this is not the case for the detector switched on the infinite past.

This clarifies and adds to the discussion on particle detectors given in [9].

## 5 Causal detector for the Dirac field

### 5.1 Minkowski space

In this section we extend the causal detector to the massless Dirac field in four-dimensional Minkowski space. The detector is still a many-level quantum mechanical system with free Hamiltonian  $H_D$ . However now the detector moves through a massless Dirac field  $\psi$  (with free Hamiltonian  $H_\psi$ ) in Minkowski space to which it is coupled via the interaction Hamiltonian

$$H_{\text{int}} = cm(\tau)\bar{\psi}(\tau)\psi(\tau), \quad (71)$$

where  $\bar{\psi} = \psi^\dagger \gamma^0$ , and  $\psi(\tau) = \psi(x(\tau))$ . The equation of motion for the free field  $\psi$  is the massless free Dirac equation  $i\gamma^\mu \partial_\mu \psi = 0$ . We choose a basis of solutions and expand the field in terms of this basis. We work throughout with the standard representation of  $\gamma$  matrices,

$$\gamma^0 = \begin{pmatrix} 1 & 0 \\ 0 & -1 \end{pmatrix}, \quad \gamma^i = \begin{pmatrix} 0 & \sigma_i \\ -\sigma_i & 0 \end{pmatrix}, \quad (72)$$

where  $\sigma_i$  are the Pauli matrices,  $\sigma_1 = \begin{pmatrix} 0 & 1 \\ 1 & 0 \end{pmatrix}$ ,  $\sigma_2 = \begin{pmatrix} 0 & -i \\ i & 0 \end{pmatrix}$  and  $\sigma_3 = \begin{pmatrix} 1 & 0 \\ 0 & -1 \end{pmatrix}$ . Then

$$\psi(t, \mathbf{x}) = \sum_{s=1,2} \int \frac{d^3 k}{(2(2\pi)^3)^{\frac{1}{2}}} \left[ b_s(\mathbf{k}) u(\mathbf{k}, s) e^{-i\omega t + i\mathbf{k}\mathbf{x}} + d_s^\dagger(\mathbf{k}) v(\mathbf{k}, s) e^{i\omega t - i\mathbf{k}\mathbf{x}} \right], \quad (73)$$

where

$$u(\mathbf{k}, 1) = \begin{pmatrix} 1 \\ 0 \\ \frac{k_z}{\omega} \\ \frac{k_+}{\omega} \end{pmatrix}, \quad u(\mathbf{k}, 2) = \begin{pmatrix} 0 \\ 1 \\ \frac{k_-}{\omega} \\ \frac{-k_z}{\omega} \end{pmatrix}, \quad (74)$$

and

$$v(\mathbf{k}, 1) = \begin{pmatrix} \frac{k_z}{\omega} \\ \frac{k_-}{\omega} \\ 1 \\ 0 \end{pmatrix}, \quad v(\mathbf{k}, 2) = \begin{pmatrix} \frac{k_-}{\omega} \\ \frac{-k_z}{\omega} \\ 0 \\ 1 \end{pmatrix}, \quad (75)$$

with  $k_{\pm} = k_x \pm ik_y$ . The modes in the expansion (73) are expressed in terms of a standard Minkowski vierbein, aligned along Minkowski coordinate axes, and they are suitably orthonormal with respect to the usual Dirac inner product in Minkowski space,

$$\langle \psi_1, \psi_2 \rangle = \int d^3x \psi_1^\dagger \psi_2 . \quad (76)$$

The free field is then quantized in the usual manner, imposing the usual anticommutation relations on the annihilation/creation operators.

We assume again that at time  $\tau_0$  the full interacting field is in the product state  $|0, E_0\rangle = |0\rangle|E_0\rangle$ . Working in the interaction picture we find, to first order in perturbation theory, that the probability that at a later time  $\tau_1 > \tau_0$  the detector is found in state  $|E_1\rangle$  is

$$\sum_{\Psi} |\langle \Psi, E_1 | 0, E_0 \rangle|^2 = c^2 |\langle E_1 | m(0) | E_0 \rangle|^2 \int_{\tau_0}^{\tau_1} d\tau \int_{\tau_0}^{\tau_1} d\tau' e^{-i\omega(\tau-\tau')} \times \langle 0 | \bar{\psi}(\tau) \psi(\tau) \bar{\psi}(\tau') \psi(\tau') | 0 \rangle , \quad (77)$$

with  $\omega = E_1 - E_0$ . Once again we shall concentrate on the response function part. With the same change of coordinates as in section 2, and differentiating with respect to  $\tau_1 = \tau$  we obtain the transition rate,

$$\dot{F}_{\tau}(\omega) = 2 \int_0^{\infty} ds \operatorname{Re} (e^{-i\omega s} \langle 0 | \bar{\psi}(\tau) \psi(\tau) \bar{\psi}(\tau-s) \psi(\tau-s) | 0 \rangle) . \quad (78)$$

Further here we find

$$\langle 0 | \bar{\psi}(\tau) \psi(\tau) \bar{\psi}(\tau') \psi(\tau') | 0 \rangle = \operatorname{Tr}((S_M^+(\tau, \tau'))^2) , \quad (79)$$

where  $\operatorname{Tr}$  is the trace and  $S_M^+(\tau, \tau') = \langle 0 | \psi(\tau) \bar{\psi}(\tau') | 0 \rangle$  is the positive frequency Wightman function, which is related to the scalar field positive frequency Wightman function by (see e.g [2])

$$S_M^+(\tau, \tau') = i\gamma^\mu \partial_\mu G_M^+(\tau, \tau') . \quad (80)$$

We note here that all expressions for the response are independent of the vierbein used to express the  $\psi$  field. This is due to the form of  $H_{\text{int}}$  (71) which is a Lorentz scalar. We also note that in the case of a massive Dirac field in Minkowski space (79) contains a second term proportional to  $\operatorname{Tr}(S_M^+(\tau, \tau'))\operatorname{Tr}(S_M^-(\tau', \tau))$ . Here in the massless case this term does not enter as  $\operatorname{Tr}(S_M^+(\tau, \tau')) = 0$  for any worldline.

Consider the uniformly accelerated worldline (9). Again a numerical calculation shows that if we use, in the scalar field correlation function above, the  $i\epsilon$  regularization we will get a  $\tau$ -dependent result for the transition rate (78) even in the  $\epsilon \rightarrow 0$  limit. We are thus led once again to consider an alternative regularization where we use a smeared form for the field operator in the interaction Hamiltonian. That is we consider

$$\psi(\tau) = \int d^3\xi W_\epsilon(\xi) S(\tau, \xi) \psi(x(\tau, \xi)) , \quad (81)$$

with the same definitions for  $W_\epsilon(\xi)$  and  $\xi$  as in section 2. In contrast to the scalar case, here we include  $S(\tau, \xi)$ , which is the spinor transformation associated with the

transformation from the Minkowski vierbein to one adapted to the Fermi-Walker coordinates. However we may now argue that in this case  $S(\tau, \xi)$  may be dropped. Firstly we note that the metric written in Fermi Walker coordinates is [1]

$$ds^2 = (1 + 2(\ddot{t}\ddot{x} - \dot{x}\ddot{t})\xi + (\ddot{x}^2 - \ddot{t}^2)\xi^2) d\tau^2 - d\xi^2. \quad (82)$$

Constant  $\tau$  spatial sections are therefore flat. It then follows that the transformation from Minkowski vierbein to that adapted to these Fermi coordinates will be independent of  $\xi$ , as Fermi Walker transport along these spatial sections in a non-rotating vierbein will be trivial. It therefore follows that  $S(\tau, \xi)$  may be taken outside the integral in (81). Further it follows from the form of  $H_{\text{int}}$  (71) that as  $S$  may be taken outside the integral it may be dropped completely. Therefore on  $M$  we may work throughout with expressions written with respect to the standard Minkowski vierbein and with

$$\psi(\tau) = \int d^3\xi W_\epsilon(\xi) \psi(x(\tau, \xi)), \quad (83)$$

as the expression for a smeared field operator. By arguments similar to those that lead to (78), the transition rate is given by

$$\dot{F}_\tau(\omega) = 2 \int_0^\infty ds \text{Re} (e^{-i\omega s} \langle 0 | \bar{\psi}(\tau) \psi(\tau) \bar{\psi}(\tau-s) \psi(\tau-s) | 0 \rangle), \quad (84)$$

and we find

$$\langle 0 | \bar{\psi}(\tau) \psi(\tau) \bar{\psi}(\tau') \psi(\tau') | 0 \rangle = \text{Tr}(\langle 0 | \psi(\tau) \bar{\psi}(\tau') | 0 \rangle^2), \quad (85)$$

where  $\psi(\tau)$  is now the smeared field (83).

Now suppose we consider again the Lorentzian profile function

$$W_\epsilon(\xi) = \frac{1}{\pi^2} \frac{\epsilon}{(\xi^2 + \epsilon^2)^2}. \quad (86)$$

The spinor correlation function is then given by

$$\begin{aligned} \langle 0 | \psi(\tau) \bar{\psi}(\tau') | 0 \rangle &= \frac{1}{2(2\pi)^3} \sum_{s=1,2} \int d^3k u(\mathbf{k}, s) u^\dagger(\mathbf{k}, s) \gamma^0 \\ &\quad \times \int d^3\xi W_\epsilon(\xi) e^{-ik \cdot x(\tau, \xi)} \int d^3\xi' W_\epsilon(\xi') e^{ik \cdot x(\tau, \xi')}. \end{aligned} \quad (87)$$

The integrals over  $\xi$  and  $\xi'$  in (87) are the same as those in (13). Proceeding as with (13), we find

$$\langle 0 | \psi(\tau) \bar{\psi}(\tau') | 0 \rangle = \frac{1}{2(2\pi)^3} \sum_{s=1,2} \int d^3k u(\mathbf{k}, s) u^\dagger(\mathbf{k}, s) \gamma^0 e^{-i\omega(t-t'-i\epsilon(t+i')) + i\mathbf{k}(\mathbf{x}-\mathbf{x}'-i\epsilon(\dot{\mathbf{x}}+\dot{\mathbf{x}}'))}. \quad (88)$$

Comparing (88) with the scalar field expression (14), with  $d = 4$  and using (74), we find we have

$$S_M^+(\tau, \tau') = \langle 0 | \psi(\tau) \bar{\psi}(\tau') | 0 \rangle = i\gamma^\mu \partial_\mu \langle 0 | \phi(\tau) \bar{\phi}(\tau') | 0 \rangle, \quad (89)$$

where  $\langle 0|\phi(\tau)\bar{\phi}(\tau')|0\rangle$  is the scalar field correlation function (14) and the partial derivative acts on the  $(t, \mathbf{x})$  but NOT on the  $(\dot{t}, \dot{\mathbf{x}})$ . Therefore we find, from (15), that the spinor correlation function is given by

$$S_M^+(\tau, \tau') = \frac{i}{4\pi^2} \frac{1}{[\tilde{t}^2 - \tilde{x}^2 - \tilde{y}^2 - \tilde{z}^2]^2} \times \begin{bmatrix} 2\tilde{t} & 0 & -2\tilde{z} & 2(i\tilde{y} - \tilde{x}) \\ 0 & 2\tilde{t} & -2(i\tilde{y} + \tilde{x}) & 2\tilde{z} \\ 2\tilde{z} & -2(i\tilde{y} - \tilde{x}) & 2\tilde{t} & 0 \\ 2(i\tilde{y} + \tilde{x}) & -2\tilde{z} & 0 & 2\tilde{t} \end{bmatrix}, \quad (90)$$

where  $\tilde{a} = (a(\tau) - a(\tau') - i\epsilon(\dot{a}(\tau) + \dot{a}(\tau')))$ . From this it is easy to show that

$$\text{Tr}(S_M^+(\tau, \tau')^2) = -\frac{1}{\pi^4} \frac{1}{((t - t' - i\epsilon(\dot{t} + \dot{t}'))^2 - (\mathbf{x} - \mathbf{x}' - i\epsilon(\dot{\mathbf{x}} + \dot{\mathbf{x}}'))^2)^3}. \quad (91)$$

### 5.1.1 Inertial detector

First we consider the response of a Dirac field detector following the inertial worldline (46) in Minkowski space. From (91), (84) and (85) the transition rate is found to be

$$\dot{F}_\tau(\omega) = -\frac{1}{\pi^4} \lim_{\epsilon \rightarrow 0} \int_{-\infty}^{\infty} ds \frac{e^{-i\omega s}}{(s - 2i\epsilon)^6}. \quad (92)$$

The integral can be done by residues, with the result

$$\dot{F}_\tau(\omega) = -\frac{\omega^5}{60\pi^3} \Theta(-\omega). \quad (93)$$

Consider also the ‘‘power spectrum’’ of the Dirac noise as defined by Takagi in [6]. The noise  $g(\tau, \tau')$  is defined by

$$g(\tau, \tau') = S(\tau)S_M^+(\tau, \tau')S(\tau')^{-1}, \quad (94)$$

where  $S(\tau) = S(\tau, \xi)$  as given in (81).  $S(\tau)$  is the spinor transformation which takes care of the Fermi-Walker transport so that  $S(\tau)\psi(\tau)$  does not rotate with respect to the detector’s proper reference frame. The definition for the power spectrum on a stationary worldline, where  $S_M^+(\tau, \tau')$  depends on  $\tau$  and  $\tau'$  only through  $\tau - \tau'$ , is

$$P(\omega) = \frac{1}{4} \text{Tr} \gamma^0 \int_{-\infty}^{\infty} d\tau e^{-i\omega\tau} g(\tau). \quad (95)$$

On the inertial trajectory (46), the transformation to the Fermi frame is trivial and we find

$$\begin{aligned} P(\omega) &= \frac{i}{2\pi^2} \int_{-\infty}^{\infty} ds \frac{e^{-i\omega s}}{(s - 2i\epsilon)^3} \\ &= \frac{\omega^2}{2\pi} \Theta(-\omega). \end{aligned} \quad (96)$$

We note that the power spectrum is  $-\omega$  times the transition rate for the linearly coupled scalar field detector following the same trajectory.

### 5.1.2 Uniformly accelerated detector

Considering once again a detector following the uniformly accelerated worldline (9). We find, as expected, that the correlation function is invariant under translations in  $\tau$  and the transition rate (84) is given by

$$\dot{F}_\tau(\omega) = -\frac{1}{64\pi^4} \lim_{\epsilon \rightarrow 0} \int_{-\infty}^{\infty} ds \frac{e^{-i\omega s}}{\left(\alpha \sinh\left(\frac{s}{2\alpha}\right) - i\epsilon \cosh\left(\frac{s}{2\alpha}\right)\right)^6}. \quad (97)$$

The integral may be done by contour integration. The result is

$$\dot{F}_\tau(\omega) = \frac{1}{60\pi^3\alpha^4} \frac{\omega}{(e^{2\pi\alpha\omega} - 1)} (4 + 5(\alpha\omega)^2 + (\alpha\omega)^4). \quad (98)$$

The response is thermal in the sense that it satisfies the KMS condition at the temperature  $T = (2\pi\alpha)^{-1}$ . It is interesting to note that there is no fermionic factor in the response, instead we have the usual Planckian factor found in the scalar case.

We can see the fermionic factor appearing however if we consider the power spectrum (95) of the Dirac noise. For the uniformly accelerated worldline we have

$$S(\tau) = \cosh\left(\frac{\tau}{2\alpha}\right) - \gamma^0\gamma^1 \sinh\left(\frac{\tau}{2\alpha}\right), \quad (99)$$

and the power spectrum (95) is given by

$$P(\omega) = \frac{i}{16\pi^2} \int_{-\infty}^{\infty} d\tau \frac{e^{-i\omega\tau}}{\left(\alpha \sinh\left(\frac{\tau}{2\alpha}\right) - i\epsilon \cosh\left(\frac{\tau}{2\alpha}\right)\right)^3}. \quad (100)$$

Again the integral may be done by contour integration to give

$$P(\omega) = \frac{1}{2\pi} \frac{\left(\omega^2 + \frac{1}{4\alpha^2}\right)}{(1 + e^{2\pi\alpha\omega})}. \quad (101)$$

Our expression here agrees with that found by Takagi [6].

## 5.2 Dirac detector for automorphic fields

Next we wish to consider this fermionic detector on  $M_0$  and  $M_-$  and in particular address the issues concerning spin structure on  $M_-$  [10]. We consider an automorphic Dirac field on Minkowski space. The main difference from the scalar case is that we must take care of what vierbeins our expressions are written with respect to. In particular our vierbein might not be invariant under the quotient group  $\Gamma$ .

We begin with a massless Dirac field  $\psi$  on  $M$ , expressed with respect to a vierbein that is invariant under  $\Gamma$ . The automorphic field is then defined by

$$\hat{\psi}(x) = \frac{1}{\left(\sum_{\gamma \in \Gamma} p(\gamma)^2\right)^{1/2}} \sum_{\gamma \in \Gamma} p(\gamma) \psi(\gamma^{-1}x), \quad (102)$$

where the normalization is such that, at equal times

$$\left\{ \hat{\psi}_\alpha(x), \hat{\psi}_\beta^\dagger(x') \right\} = \delta^{(d-1)}(x - x') \delta_{\alpha\beta} + \text{image terms}. \quad (103)$$

The two-point function for the automorphic field is then given by the method of images,

$$S_{M/\Gamma}^+(x, x') = \langle 0 | \hat{\psi}(x) \bar{\hat{\psi}}(x') | 0 \rangle = \sum_{\gamma \in \Gamma} p(\gamma) \langle 0 | \psi(x) \bar{\psi}(\gamma^{-1}x') | 0 \rangle . \quad (104)$$

We consider a detector coupled to the automorphic field via the interaction Hamiltonian

$$H_{\text{int}} = cm(\tau) \bar{\hat{\psi}}(\tau) \hat{\psi}(\tau) , \quad (105)$$

where

$$\hat{\psi}(\tau) = \int d^3\xi W_\epsilon(\xi) S(\tau, \xi) \hat{\psi}(x(\tau, \xi)) . \quad (106)$$

The transition rate is given by

$$\dot{F}_\tau(\omega) = 2 \int_0^\infty ds \text{Re} \left( e^{-i\omega s} \langle 0 | \bar{\hat{\psi}}(\tau) \hat{\psi}(\tau) \bar{\hat{\psi}}(\tau-s) \hat{\psi}(\tau-s) | 0 \rangle \right) . \quad (107)$$

Further we may show, with a calculation similar to that leading to (79) and (85), that

$$\langle 0 | \bar{\hat{\psi}}(\tau) \hat{\psi}(\tau) \bar{\hat{\psi}}(\tau') \hat{\psi}(\tau') | 0 \rangle = \text{Tr} \left( \langle 0 | \hat{\psi}(\tau) \bar{\hat{\psi}}(\tau') | 0 \rangle^2 \right) , \quad (108)$$

with

$$\langle 0 | \hat{\psi}(\tau) \bar{\hat{\psi}}(\tau') | 0 \rangle = \sum_{\gamma \in \Gamma} p(\gamma) \langle 0 | \psi(\tau) \bar{\psi}(\gamma^{-1}\tau') | 0 \rangle . \quad (109)$$

Therefore the method of images may be directly applied to our Minkowski space correlation functions here.

It is important to note that the above mode sum expressions are changed when considering a vierbein not invariant under the action of  $\Gamma$ . Suppose we consider two vierbeins, one invariant under  $\Gamma$  (labelled by an  $I$ ) and another not invariant (labelled by  $N$ ). In the vierbein  $I$  the automorphic field is given by the mode sum expression (102). The transformation from  $I$  to  $N$  will transform the spinors as  $\hat{\psi}_I(x) \rightarrow \hat{\psi}_N(x) = S(x) \hat{\psi}_I(x)$ . Then from (102)

$$\hat{\psi}_N(x) = \frac{1}{\left( \sum_{\gamma \in \Gamma} p(\gamma)^2 \right)^{1/2}} \sum_{\gamma \in \Gamma} p(\gamma) S(x) \psi_I(\gamma^{-1}x) , \quad (110)$$

and hence the mode sum expression for the automorphic field in terms of the non-invariant vierbein is

$$\hat{\psi}_N(x) = \frac{1}{\left( \sum_{\gamma \in \Gamma} p(\gamma)^2 \right)^{1/2}} \sum_{\gamma \in \Gamma} p(\gamma) S(x) S^{-1}(\gamma^{-1}x) \psi_N(\gamma^{-1}x) . \quad (111)$$

Similarly the two-point function transforms as

$$S_{IM/\Gamma}^+(x, x') \rightarrow S_{NM/\Gamma}^+(x, x') = S(x) S_{IM/\Gamma}^+(x, x') S^{-1}(x') . \quad (112)$$

From (104), the mode sum expression for the two point function in terms of the non-invariant vierbein is hence

$$\begin{aligned} S_{NM/\Gamma}^+(x, x') &= \sum_{\gamma \in \Gamma} p(\gamma) S(x) \langle 0 | \psi_I(x) \bar{\psi}_I(\gamma^{-1}x') | 0 \rangle S^{-1}(x') , \\ &= \sum_{\gamma \in \Gamma} p(\gamma) \langle 0 | \psi_N(x) \bar{\psi}_N(\gamma^{-1}x') | 0 \rangle S^{-1}(\gamma^{-1}x') S^{-1}(x') . \end{aligned} \quad (113)$$

In sections 5.3 and 5.4 we shall work throughout in vierbeins invariant under  $J_0$  and  $J_-$  respectively.

### 5.3 Dirac detector on $M_0$

Consider now Dirac field theory on  $M_0$  as an automorphic field theory on  $M$  where expressions are written with respect to the standard Minkowski vierbein. From (109) the  $M_0$  correlation function is given by

$$S_{M_0}^+(\tau, \tau') = \sum_{n \in \mathbb{Z}} \eta^n S_M^+(\tau, J_0(\tau')) , \quad (114)$$

where  $\eta = 1, (-1)$  labels spinors with periodic (antiperiodic) boundary conditions. We therefore find an explicit expression for  $S_{M_0}^+(\tau, \tau')$  from (114) and (90). As we work throughout in the standard Minkowski vierbein here, writing the smeared field operator as in (106), we may again argue in an analogous way to in the previous section that the spinor transformation  $S(\tau, \xi)$  can be dropped.

#### 5.3.1 Inertial detector

First consider a Dirac detector following the inertial worldline (46) on  $M_0$ . The power spectrum (95) for the noise is found to be

$$P(\omega) = \left( \frac{\omega^2}{2\pi} + 2 \sum_{n=1}^{\infty} \frac{\eta^n \omega}{4\pi n a} \sin(2n\omega a) \right) \Theta(-\omega) . \quad (115)$$

As on Minkowski space the power spectrum is  $-\omega$  times the transition rate of the linearly coupled scalar field detector following the same trajectory (38). The summation thus may be performed to give  $-\omega$  times (39) and (40).

For the transition rate we find

$$\dot{F}_\tau(\omega) = -\frac{1}{\pi^4} \sum_{n \in \mathbb{Z}} \sum_{m \in \mathbb{Z}} \int_{-\infty}^{\infty} ds \frac{\eta^n \eta^m ((s - 2i\epsilon)^2 - 4nma^2)}{[(s - 2i\epsilon)^2 - (2na)^2]^2 [(s - 2i\epsilon)^2 - (2ma)^2]^2} . \quad (116)$$

The  $n = 0, m = 0$  term gives the transition rate on Minkowski space (93). The integral for other terms may be done by residues, with the result

$$\begin{aligned} \dot{F}_\tau(\omega) &= \left( -\frac{\omega^5}{60\pi^3} + \frac{1}{32\pi} \sum_{\substack{n, m = -\infty \\ n, m \neq 0}}^{\infty} \frac{\eta^n \eta^m}{(m - n)(m + n)^3 a^5} \left[ \left( \left( \frac{2m\omega a}{n} + 2\omega a \right) \cos(2\omega n a) \right. \right. \right. \right. \\ &\quad \left. \left. \left. \left. - \frac{(m + 3n)}{n^2} \sin(2\omega n a) \right) + \left( \left( \frac{2\omega a n}{m} + 2\omega a \right) \cos(2\omega m a) \right. \right. \right. \\ &\quad \left. \left. \left. - \frac{(n + 3m)}{m^2} \sin(2\omega m a) \right) \right] \right) \Theta(-\omega) , \end{aligned} \quad (117)$$

where the  $n = m$  and  $n = -m$  terms are understood in the limiting sense and can be verified to be finite. As expected the response does not depend on the velocity.

### 5.3.2 Uniformly accelerated detector

Next consider the power spectrum for the Rindler noise, that is we consider  $g(\tau, \tau')$  on the uniformly accelerated worldline. From (95) we find

$$P(\omega) = \frac{i}{16\pi^2} \int_{-\infty}^{\infty} d\tau \sum_{n \in \mathbb{Z}} \frac{\eta^n e^{-i\omega\tau} (\alpha \sinh(\frac{\tau}{2\alpha}) - i\epsilon \cosh(\frac{\tau}{2\alpha}))}{\left((\alpha \sinh(\frac{\tau}{2\alpha}) - i\epsilon \cosh(\frac{\tau}{2\alpha}))^2 - (na)^2\right)^2}. \quad (118)$$

The contributions to the integral from each term in the sum may be calculated separately by contour integration. The result is

$$\begin{aligned} P(\omega) = & \frac{1}{2\pi} \frac{(\omega^2 + \frac{1}{4\alpha^2})}{(1 + e^{2\pi\alpha\omega})} \\ & + 2 \sum_{n=1}^{\infty} \frac{\eta^n}{(1 + e^{2\pi\alpha\omega})} \left[ \frac{\alpha^2 n^2 a^2 \cos\left(2\omega\alpha \operatorname{arctanh}\left(\frac{(\alpha^2 n^2 a^2 + n^4 a^4)^{1/2}}{\alpha^2 + n^2 a^2}\right)\right)}{4\pi \left(\frac{\alpha^2}{\alpha^2 + n^2 a^2}\right)^{1/2} (2n^6 a^6 + 4n^4 a^4 \alpha^2 + 2n^2 a^2 \alpha^4)} \right. \\ & \left. + \frac{\alpha^3 (\alpha^2 n^2 a^2 + n^4 a^4)^{1/2} \omega \sin\left(2\omega\alpha \operatorname{arctanh}\left(\frac{(\alpha^2 n^2 a^2 + n^4 a^4)^{1/2}}{\alpha^2 + n^2 a^2}\right)\right)}{2\pi \left(\frac{\alpha^2}{\alpha^2 + n^2 a^2}\right)^{1/2} (2n^6 a^6 + 4n^4 a^4 \alpha^2 + 2n^2 a^2 \alpha^4)} \right] \end{aligned} \quad (119)$$

where again  $\eta$  labels the spin structure. We see that the power spectrum depends on the spin structure. The  $n = 0$  term in (119) agrees with the Minkowski space power spectrum (101) as expected, and both the  $n = 0$  and  $n > 0$  terms in (119) contain the fermionic factor. Note that no simple relation holds between the power spectrum (119) and the transition rate of the linearly coupled scalar field detector (41), in contrast to the relation we observed on the inertial worldline.

For the transition rate of a fermionic detector on  $M_0$  we have

$$\dot{F}_\tau(\omega) = 2 \int_0^\infty ds \operatorname{Re} \left( e^{-i\omega s} \operatorname{Tr} \left( S_{M_0}^+(\tau, \tau - s)^2 \right) \right). \quad (120)$$

We may evaluate (120) on the uniformly accelerated worldline by substituting the worldline into (114) and (89). It is easy to show that the  $n = 0$  term leads to the transition rate found on Minkowski space (98) as expected. The evaluation of the other terms is not so straightforward as the residues are not so easy to calculate. We shall not present the result here.

### 5.4 Dirac detector on $M_-$

On  $M_-$  we can again build expressions from those on  $M$  (or  $M_0$ ) via the method of images. The transition rate is given by

$$\dot{F}_\tau(\omega) = 2 \int_0^\infty ds \operatorname{Re} \left( e^{-i\omega s} \operatorname{Tr} \left( S_{M_-}^+(\tau, \tau - s)^2 \right) \right), \quad (121)$$

and

$$S_{M_-}^+(\tau, \tau') = S_{M_0}^+(\tau, \tau') + \rho S_{M_0}^+(\tau, J_-(\tau')) , \quad (122)$$

$$= \sum_{n \in \mathbb{Z}} \rho^n S_M^+(\tau, J_-^n(\tau')) , \quad (123)$$

where  $S_{M_0}^+(\tau, \tau')$  and  $S_M^+(\tau, \tau')$  are written in terms of a vierbein which rotates by  $2\pi$  in the  $(x, y)$ -plane as  $z \mapsto z + 2a$  (i.e. the one spin structure on  $M_0$  compatible with the two on  $M_-$  [10]).  $\rho = 1(-1)$  labels spinors with periodic (antiperiodic) boundary conditions on  $M_-$  with respect to this vierbein. That is  $\rho$  labels the two possible spin structures on  $M_-$ .

Now on  $M_-$  our main question of interest is whether or not our detector can distinguish the two possible spin structures. The stress tensor for the massless spinor field in  $M_-$  [10] has non-zero shear components,  $\langle 0_- | T_{xz} | 0_- \rangle$  and  $\langle 0_- | T_{yz} | 0_- \rangle$ , which change sign under a change of spin structure. It is therefore conceivable that a detector with a non-zero  $z$ -component of angular momentum could detect the spin structure. However as the relation between  $\langle 0_- | T_{\mu\nu} | 0_- \rangle$  and the detector response is not clear it is not possible to tell in advance whether or not our detector model will be sensitive to the spin structure.

We consider therefore a detector following the trajectory

$$t = t(\tau) , \quad x = x(\tau) , \quad y = y_0 , \quad z = z_0 , \quad (124)$$

where  $y_0 \neq 0$  and  $z_0$  are constants. First we note that there is no direct analogue of the Rindler noise power spectrum here as the power spectrum is defined in [6] only for stationary trajectories. We therefore look directly at the transition rate. From (122) and (121) the transition rate will contain four terms. The first term, coming from  $\text{Tr} \left( S_{M_0}^+(\tau, \tau') \right)^2$ , will give us the same response as on  $M_0$  (for  $\eta = -1$  in (114), as these expressions are written with respect to the standard Minkowski vierbein). This part is independent of spin structure ( $\rho$ ) on  $M_-$ . The fourth term, coming from  $\text{Tr} \left( \left( \rho S_{M_0}^+(\tau, J_-(\tau')) \right)^2 \right)$ , will also be independent of spin structure, as it contains only  $\rho^2 = 1$  in both cases. Thus the only way in which the transition rate may be sensitive to the spin structure on  $M_-$  is through the cross terms,  $\text{Tr}(\rho S_{M_0}^+(\tau, J_-(\tau')) S_{M_0}^+(\tau, \tau'))$  and  $\text{Tr}(\rho S_{M_0}^+(\tau, \tau') S_{M_0}^+(\tau, J_-(\tau')))$ . However it is a reasonably straightforward matter to show that these traces are both 0 on the trajectory (124), due to simple cancellations in the products of the Wightman functions. Thus we see, even without an explicit calculation on a specific trajectory, that the transition rate cannot depend on  $\rho$ , and so the detector is not sensitive to the spin structure, for *any* motion at constant  $y$  and  $z$ .

Unfortunately an explicit evaluation of the transition rate on the inertial or uniformly accelerated worldlines, as on  $M_0$ , is difficult to obtain and we shall not discuss it further here.

## 6 Static detectors on the $\mathbb{RP}^3$ geon

In the recent literature Deser and Levin [24, 26, 45] have presented kinematical arguments for the calculation of the Hawking-Unruh effects in a large class of black hole

and cosmological spaces by mapping the trajectories of detectors in these spacetimes to Rindler trajectories in higher dimensional embedding spaces (known as GEMS, or global embedding Minkowski spacetimes) in which these spacetimes have global embeddings. In [26] uniformly accelerated observers in de Sitter and Anti de Sitter space are considered. It is seen that in de Sitter space their experience is thermal with temperature  $T = a_5/(2\pi)$  where  $a_5$  is their associated acceleration in the 5-dimensional embedding space. In Anti de Sitter space their experience is thermal provided the acceleration is above a certain threshold. In [45] static observers in Schwarzschild space are considered via a 6-dimensional flat embedding space and the expected temperature and entropy are recovered. In [24] this GEMS approach for the derivations of temperature and entropy is extended to Schwarzschild-(anti) de Sitter and Reissner-Nordström spaces in four dimensions and rotating BTZ spaces in three dimensions, and the methods of [24] can be readily adapted to other cases. We note that indeed any Einstein geometry has a GEMS [46].

[47] considers GEMS calculations on a large class of higher dimensional black holes, generalising the four-dimensional results of Deser and Levin (and the results for the four-dimensional AdS hole and others in [48]). In particular,  $d$ -dimensional Schwarzschild and Reissner-Nordstrom in asymptotically flat, de Sitter and Anti de Sitter spaces are discussed. The case of four-dimensional asymptotically locally anti-de Sitter is particularly interesting as solutions with planar, cylindrical, toroidal and hyperbolic horizon topology exist. The higher dimensional versions of these non-spherical AdS black holes are also considered. Their global embeddings in higher dimensional Minkowski spaces are found and the associated temperatures and entropies obtained. Other references on GEMS come from the group of Hong, Park, Kim, Soh and Oh [48–52]. These include the 4-dimensional AdS hole as mentioned above, static rotating and charged BTZ holes,  $(2+1)$  de Sitter holes, scalar tensor theories, charged dilatonic black holes in  $1+1$  dimensions, charged and uncharged black strings in  $(2+1)$  dimensions, and a few other cases. A recent paper by Chen and Tian [53] argues that the GEMS approach holds for general stationary motions in curved spacetimes. However these authors argue further that the approach in general fails for non-stationary motions. The example they use is that of a freely falling observer in the Schwarzschild geometry. We note here that although their argument does prove that the GEMS argument is not valid for some non-stationary trajectories by use of an example, it does not prove that the GEMS approach is useless for all such trajectories.

Within the kinematical arguments employed in all the work reviewed above the great simplification in working with these GEMS is that we are mapping situations in curved spacetimes to corresponding ones in a flat spacetime, where calculations are always simpler, both conceptually and technically. It seems reasonable following the success of the GEMS programme that the responses of particle detectors in black hole and cosmological backgrounds could also be related in some way to responses of corresponding detectors in their GEMS. We note immediately that such a mapping of detector responses is clearly not trivial as we would expect different responses to occur due to the different dimensions which the spacetimes and their GEMS have, however some relation is still expected. In this section then we present an argument which should be relevant to the response of a static detector in the single exterior of the  $\mathbb{RP}^3$  geon black hole (and the Kruskal spacetime) via an embedding of the

Kruskal manifold into a 7-dimensional Minkowski space. This embedding space is different to the 6-dimensional embedding of Kruskal so far used in the GEMS literature [54], but we use it as it is more easily adapted to the  $\mathbb{RP}^3$  geon.

We begin by first presenting the embedding (see [25]). The complexified Kruskal manifold  $M_C$  here is considered to be an algebraic variety in  $\mathbb{C}^7$ . With coordinates  $(z_1, \dots, z_7)$  and metric

$$ds^2 = -(dz_1)^2 - (dz_2)^2 - \dots - (dz_6)^2 + (dz_7)^2 , \quad (125)$$

$z_7$  being the timelike coordinate,  $M_C$  is determined by

$$\begin{aligned} (z_6)^2 - (z_7)^2 + 4/3(z_5)^2 &= 16M^2 , \\ ((z_1)^2 + (z_2)^2 + (z_3)^2)(z_5)^4 &= 576M^6 , \\ \sqrt{3}z_4z_5 + (z_5)^2 &= 24M^2 . \end{aligned} \quad (126)$$

The Lorentzian section of  $M_C$ , denoted by  $\hat{M}_L$ , is the subset stabilised by  $J_L : (z_1, \dots, z_7) \mapsto (z_1^*, \dots, z_7^*)$ , where  $*$  stands for complex conjugation.  $\hat{M}_L$  consists of two connected components, one with  $z_5 > 0$  and one  $z_5 < 0$ , both of which are isometric to the Kruskal manifold, which we denote by  $M_L$ . An explicit embedding of  $M_L$  into  $\hat{M}_L$  with  $z_5 > 0$  is given by

$$\begin{aligned} z_1 &= r \sin \theta \cos \phi , \\ z_2 &= r \sin \theta \sin \phi , \\ z_3 &= r \cos \theta , \\ z_4 &= 4M \left( \frac{r}{2M} \right)^{1/2} - 2M \left( \frac{2M}{r} \right)^{1/2} , \\ z_5 &= 2M \left( \frac{6M}{r} \right)^{1/2} , \\ z_6 &= 4M \left( \frac{2M}{r} \right)^{1/2} \exp \left( -\frac{r}{4M} \right) X , \\ z_7 &= 4M \left( \frac{2M}{r} \right)^{1/2} \exp \left( -\frac{r}{4M} \right) T , \end{aligned} \quad (127)$$

with  $X^2 - T^2 > -1$  and  $r = r(T, X)$  defined as the unique solution to

$$\left( \frac{r}{2M} - 1 \right) \exp \left( \frac{r}{2M} \right) = X^2 - T^2 . \quad (128)$$

Here  $(T, X, \theta, \phi)$  are a set of usual Kruskal coordinates, giving the usual Kruskal metric on  $M_L$ . In each of the four regions of  $M_L$ ,  $|X| \neq |T|$ , one can introduce as usual local Schwarzschild coordinates  $(t, r, \theta, \phi)$ . For  $X > |T|$ , the transformation reads

$$\begin{aligned} T &= \left( \frac{r}{2M} - 1 \right)^{1/2} \exp \left( \frac{r}{4M} \right) \sinh \left( \frac{t}{4M} \right) , \\ X &= \left( \frac{r}{2M} - 1 \right)^{1/2} \exp \left( \frac{r}{4M} \right) \cosh \left( \frac{t}{4M} \right) , \end{aligned} \quad (129)$$

where  $r > 2M$ , and the expressions for  $z_1, z_2, \dots, z_5$  are as in (127) while those for  $z_6$  and  $z_7$  become

$$\begin{aligned} z_6 &= 4M \left(1 - \frac{2M}{r}\right)^{1/2} \cosh\left(\frac{t}{4M}\right), \\ z_7 &= 4M \left(1 - \frac{2M}{r}\right)^{1/2} \sinh\left(\frac{t}{4M}\right). \end{aligned} \quad (130)$$

Recalling that  $z_7$  is the timelike coordinate in the embedding space, we see immediately that an observer static in the exterior region  $X > |T|$  at  $r = \text{const}, \theta = \text{const}, \phi = \text{const}$  is a Rindler observer in the 7-dimensional embedding space with  $(z_1, \dots, z_5)$  constant and acceleration in the  $z_6$ -direction of magnitude

$$a = 1/\alpha = \frac{1}{4M \left(1 - \frac{2M}{r}\right)^{1/2}}. \quad (131)$$

As we have seen, the response of such a Rindler detector in the embedding space is thermal with the associated temperature

$$T = \frac{a}{2\pi} = \frac{1}{2\pi\alpha} = \frac{1}{8\pi M \left(1 - \frac{2M}{r}\right)^{1/2}}. \quad (132)$$

This gives the Hawking temperature as seen by the static observer in the black hole spacetime. The associated black hole temperature, i.e. the temperature as seen at infinity, in the Kruskal spacetime is given by the Tolman relation

$$T_0 = g_{00}^{1/2} T = \frac{1}{8\pi M}, \quad (133)$$

(132) and (133) are the expected expressions on Kruskal space [2]. Thus the black hole temperature as seen by a static observer has been derived from the Unruh temperature seen by the associated Rindler observer in the global embedding Minkowski spacetime.

Next we consider the  $\mathbb{RP}^3$  geon. This is built as a quotient of the Kruskal manifold under the involutive isometry  $J_G : (T, X, \theta, \phi) \mapsto (T, -X, \pi - \theta, \phi + \pi)$ . We now extend the action of the group generated by  $J_G$  to the 7-dimensional embedding space  $M_C$  in order to obtain a suitable embedding space for the geon. A suitable extension of  $J_G$  is  $\bar{J}_G : (z_1, z_2, z_3, z_4, z_5, z_6, z_7) \mapsto (-z_1, -z_2, -z_3, z_4, z_5, -z_6, z_7)$ , which is an involution on  $M_C$ . Again the worldline of a static detector in the  $\mathbb{RP}^3$  geon exterior  $X > |T|$  is mapped to the worldline of a Rindler observer with acceleration in the  $z_6$ -direction with magnitude (131) in this embedding space. We suggest therefore that the calculations of the time dependent responses of an accelerated observer in the  $d$ -dimensional quotients of Minkowski space, done in section 4.3, should have relevance to the response of a static detector in the exterior of the  $\mathbb{RP}^3$  geon (although the exact nature of the relationship is not clear). In particular if we specialise the results of section 4.3 to a detector with uniform acceleration (131) in the quotient of a 7-dimensional Minkowski space under involution  $\bar{J}_G$  we see that the response has two parts. The thermal time-independent part is given by (19), which in the present case reads

$$\dot{F}_{M\tau}(\omega) = \frac{a^4}{64\pi^2(e^{\frac{2\pi\omega}{a}} + 1)} (1/4 + \omega^2/a^2)(9/4 + \omega^2/a^2). \quad (134)$$

Again this is a thermal response associated with a temperature  $T = \frac{a}{2\pi}$ . Clearly the response is different to that of the static detector on Kruskal due to the higher number of dimensions though the two should be related. The image part of the response for this Rindler detector is, in the case of a detector switched on in the infinite past,

$$\dot{F}_{I\tau}(\omega) = \frac{3}{8\pi^3} \int_0^\infty ds \frac{\cos(\omega s)}{\left(\frac{4}{a^2} \cosh^2\left(\frac{a(2\tau-s)}{2}\right) + 4r^2\right)^{5/2}}. \quad (135)$$

The total response for certain values of the parameters is shown in figure 8. The

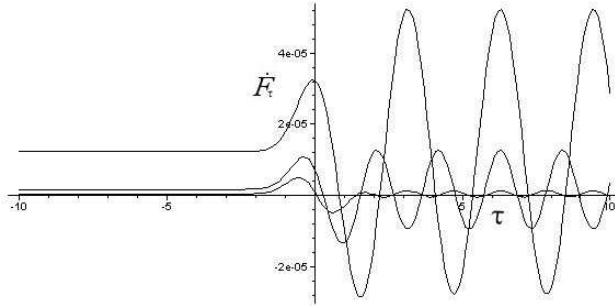


Figure 8: Transition rate for a detector uniformly accelerated in the  $z_1$  direction on the quotient of 7-dimensional Minkowski space under the involution  $\bar{J}_G$ . The parameters are  $\alpha = 1$ ,  $C = (2z_1)^2 + (2z_2)^2 + (2z_3)^2 = 4r^2 = 64/9$ , and  $\omega = 1$  (upper curve),  $\omega = 1.5$  and  $\omega = 2$  (lower curve).

comments of section 4.2.2 then follow. The image part consists of a term periodic in  $\tau$  with period  $\pi/\omega$  plus a term bounded by a function which dies off exponentially for large  $\tau$ . The numerical evidence exhibits behaviour qualitatively very similar to that of figure 4. The comments made in the section 4.2.2 about finite time detections also follow here. In particular the oscillatory behaviour of the boundary part as  $\tau \rightarrow \infty$  is a property only of the case of infinite time detection. For a detector switched on at  $-\infty < \tau_0 < 0$  the transition rate oscillates for some time period with  $\tau > 0$ , but eventually it will fall to the thermal response and so at late times the difference between the response on the Minkowski space and that on the quotient space vanishes. That is, for instantaneous, exponential and Gaussian switching the image term behaves qualitatively as shown in figures 5, 6 and 7, respectively. This implies for finite time static detectors on the  $\mathbb{RP}^3$  geon the difference between the response there and that on Kruskal spacetime falls off also to 0 at late times, which is in agreement with the comments made in [9]. Note however the different behaviour in the case of the infinite time detection.

## 7 De Sitter and $\mathbb{RP}^3$ de Sitter spaces

In this section we begin in subsection 7.1 by considering a model detector in de Sitter space. Throughout we consider a conformally coupled massless scalar field

moving through the Euclidean vacuum [55]. We see that here a similar situation is encountered to that found by Schlicht for the uniformly accelerated detector in Minkowski space. It is seen that in the case of a comoving detector switched on in the infinite past and off at finite  $\tau$ , if the correlation function is regularized by a naive  $i\epsilon$ -prescription, as for example is done in Birrell and Davies [2], we are led to an unphysical,  $\tau$ -dependent response. We therefore introduce an alternative regularization. Further, for a comoving detector, we show that such a regularization can arise also by considering a model detector with spatial extent, that is by considering a smeared field operator in the interaction Hamiltonian. We recover the usual time independent thermal response for comoving and uniformly accelerated detectors.

Subsection 7.2 then considers comoving observers in  $\mathbb{RP}^3$  de Sitter space, such that the motion is orthogonal to the distinguished foliation [11]. In addition to the thermal part seen in de Sitter space, the transition rate contains an image part, related to that found in section 4.2 for a uniformly accelerated detector on a four-dimensional Minkowski space with a planar boundary. We also address a comoving detector in de Sitter and  $\mathbb{RP}^3$  de Sitter space in a GEMS approach, by considering the response of the associated uniformly accelerated detectors in higher dimensional Minkowski (with boundaries in the case of  $\mathbb{RP}^3$  de Sitter) embedding spaces. As we are able to do the calculations both in the original curved spaces and in the global embedding spaces, the results help to clarify the relation and validity of relating detector responses to those in embedding spaces.

## 7.1 Detectors in de Sitter space

We represent  $d$ -dimensional de Sitter space as the hyperboloid

$$z_0^2 - z_1^2 - \cdots - z_d^2 = -\alpha^2 , \quad (136)$$

embedded in the  $d + 1$ -dimensional Minkowski space,

$$ds^2 = dz_0^2 - dz_1^2 - \cdots - dz_d^2 , \quad (137)$$

with  $z_i$  real-valued coordinates. Let us consider the coordinates  $(t, \mathbf{x})$  defined by

$$\begin{aligned} z_0 &= \alpha \sinh(t/\alpha) + \frac{e^{t/\alpha}}{2\alpha} |\mathbf{x}|^2 , \\ z_d &= \alpha \cosh(t/\alpha) - \frac{e^{t/\alpha}}{2\alpha} |\mathbf{x}|^2 , \\ z_i &= e^{t/\alpha} x_i . \end{aligned} \quad (138)$$

These coordinates cover the half of the de Sitter hyperboloid given by  $z_0 + z_d > 0$ . The line element is that of a  $d$ -dimensional Friedman-Robertson-Walker spacetime with exponentially expanding flat spatial sections,

$$ds^2 = dt^2 - e^{2t/\alpha} (dx_1^2 + \cdots + dx_{d-1}^2) . \quad (139)$$

Introducing the conformal time  $\eta = -\alpha e^{-t/\alpha}$ , the line element becomes conformal to Minkowski space,

$$ds^2 = \frac{\alpha^2}{\eta^2} \left[ d\eta^2 - \sum_{i=1}^{d-1} (dx_i)^2 \right] , \quad (140)$$

where  $-\infty < \eta < 0$ .

Consider a massless conformally coupled scalar field in the line element (140). A complete set of mode solutions to the Klein-Gordon equation positive frequency with respect to conformal Killing time  $\eta$  is given by [2]

$$\phi_{\mathbf{k}}(\eta, \mathbf{x}) = \frac{\eta^{d/2-1}}{(2\alpha^{d-2}\omega(2\pi)^{d-1})^{1/2}} e^{-i\omega\eta+i\mathbf{k}\cdot\mathbf{x}}. \quad (141)$$

The field may be expanded in the modes (141) and quantized in the usual way. The associated vacuum state, that is the conformal vacuum, coincides with the state known as the Euclidean vacuum [2]. The Euclidean vacuum  $|0_E\rangle$  is uniquely characterised as the state whose correlation function  $\langle 0_E|\phi(x)\phi(x')|0_E\rangle$  is invariant under the connected component of the de Sitter group, and the only singularities of the correlation function are when  $x'$  is on the lightcone of  $x$  [55]. Even though we have here defined the Euclidean vacuum in coordinates that only cover half of the de Sitter hyperboloid, it is worth mentioning that the state is well defined on the whole hyperboloid [2].

We now consider a monopole detector linearly coupled to the field via the interaction Hamiltonian

$$H_{\text{int}} = cm(\tau)\phi(x(\tau)). \quad (142)$$

The transition rate, for a detector originally in state  $|E_0\rangle$  with the field in the Euclidean vacuum state at time  $\tau_0$ , to be found in the state  $|E_1\rangle$  at time  $\tau > \tau_0$  is then, to first order in perturbation theory

$$\dot{F}_\tau(\omega) = 2 \int_0^{\tau-\tau_0} ds \text{Re} \left( e^{-i\omega s} \langle 0_E|\phi(\tau)\phi(\tau-s)|0_E\rangle \right), \quad (143)$$

where  $\omega = E_1 - E_0$ . The correlation function  $\langle 0_E|\phi(x)\phi(x')|0_E\rangle$  from (141) is given by

$$\begin{aligned} \langle 0_E|\phi(x(\tau))\phi(x(\tau'))|0_E\rangle &= \frac{(\eta\eta')^{d/2-1}}{\alpha^{d-2}(2\pi)^{d-1}} \\ &\times \int \frac{d^{d-1}k}{2|\mathbf{k}|} e^{-i|\mathbf{k}|(\eta(\tau)-\eta(\tau'))+i\mathbf{k}\cdot(\mathbf{x}(\tau)-\mathbf{x}(\tau'))}. \end{aligned} \quad (144)$$

(144) is conformally related to the Minkowski space Wightman function by

$$\langle 0_E|\phi(x)\phi(x')|0_E\rangle = \left(\frac{\eta}{\alpha}\right)^{d/2-1} \langle 0|\phi(x)\phi(x')|0\rangle \left(\frac{\eta'}{\alpha}\right)^{d/2-1}. \quad (145)$$

The integrals in (144) may be performed by transforming to hyperspherical coordinates. The integral over  $|\mathbf{k}|$  requires regularization.

We shall now specialize to four-dimensional de Sitter space (although the extension to higher dimensions is straightforward). If we regularize (144) with a naive  $i\epsilon$ -prescription, that is, we introduce the cut-off  $e^{-\epsilon\omega}$ , we find via a numerical calculation that the transition rate (143) for a comoving detector with worldline  $t = \tau$ ,  $\mathbf{x} = 0$ , when the detector is switched on at  $\tau = -\infty$  and off at  $\tau$ , is time dependent and therefore apparently unphysical. We are led, as was Schlicht with the uniformly

accelerated detector in Minkowski space, to an alternative regularization of (144). Our proposal is to consider the correlation function with the relation (145) to the Minkowski space correlation function of Schlicht [1]. That is

$$\begin{aligned} \langle 0_E | \phi(\tau) \phi(\tau') | 0_E \rangle &= -\frac{1}{4\pi^2 \alpha^2} \frac{\eta(\tau) \eta'(\tau)}{A} \\ A &= [(\eta(\tau) - \eta(\tau') - i\epsilon(\dot{\eta}(\tau) + \dot{\eta}(\tau'))^2 - (\mathbf{x}(\tau) - \mathbf{x}(\tau') - i\epsilon(\dot{\mathbf{x}}(\tau) + \dot{\mathbf{x}}(\tau')))^2], \end{aligned} \quad (146)$$

with the transition rate still given by (143).

Consider a uniformly accelerated detector following the worldline

$$\begin{aligned} z_0 &= \alpha \sinh(t/\alpha) + \frac{e^{-t/\alpha}}{2\alpha} r^2, \\ z_4 &= \alpha \cosh(t/\alpha) - \frac{e^{-t/\alpha}}{2\alpha} r^2, \\ z_1 &= z_2 = 0, \\ z_3 &= r, \end{aligned} \quad (147)$$

with  $r = \text{constant}$ . The worldline of such an observer in the embedding space is a hyperbola  $(z_4)^2 - (z_0)^2 = \alpha^2 - r^2$ ,  $z_1 = z_2 = 0$ ,  $z_3 = r$ . In the de Sitter space the observer has constant proper acceleration  $a$ , where  $a^2 = -g_{\mu\nu} \dot{u}^\mu \dot{u}^\nu$ ,  $\dot{u}^\mu = u^\nu (\nabla_\nu u^\mu)$  and  $u^\mu$  is the tangent vector of the trajectory, of magnitude

$$a = \frac{r}{\alpha(\alpha^2 - r^2)^{1/2}}. \quad (148)$$

The proper time for the accelerated observer is  $\tau = (\alpha^2 - r^2)^{1/2} t/\alpha$ .

Substituting (147) into (146) we find

$$\langle 0_E | \phi(\tau) \phi(\tau') | 0_E \rangle = -\frac{1}{16\pi^2 \left( (\alpha^2 - r^2)^{1/2} \sinh \left( \frac{\tau - \tau'}{2(\alpha^2 - r^2)^{1/2}} \right) - i\epsilon \cosh \left( \frac{\tau - \tau'}{2(\alpha^2 - r^2)^{1/2}} \right) \right)^2}, \quad (149)$$

and from (143) the transition rate of the detector switched on in the infinite past and off at time  $\tau$  is independent of  $\tau$  and is given by

$$\dot{F}_\tau(\omega) = \frac{\omega}{2\pi(e^{2\pi\omega(\alpha^2 - r^2)^{1/2}} - 1)}. \quad (150)$$

The accelerated detector thus experiences a thermal response at temperature

$$T = \frac{1}{2\pi} \left( \frac{1}{\alpha^2} + a^2 \right)^{1/2}. \quad (151)$$

The response of a comoving detector is obtained by setting  $a = 0$ . The transition rate is still thermal at temperature  $T = 1/(2\pi\alpha)$ . These results agree with the previous literature (e.g [2, 26]). What is new is that we have obtained these results in a causal way for a detector switched on in the infinite past and read at a finite time, as opposed to the case usually considered of a detection over the entire worldline.

We end this section by showing that the regularization in (146), in the case of a comoving observer, may be obtained by considering the monopole detector as the

limit of an extended detector in de Sitter space. The reason why this is simple in the case of a comoving observer but not for other trajectories is that spatial hypersurfaces of constant  $t$  in the coordinates  $(t, \mathbf{x})$  are flat Euclidean spaces, which allow us to introduce a detector with infinite spatial extent along these slices. Care must be taken when defining the shape function for the detector however, because the hypersurfaces are expanding with increasing  $t$ , with a shape which is rigid in the proper distance the regularization follows. The averaging over spatial hypersurfaces in effect introduces a short distance, high frequency cut-off in the modes.

The detector model is that of section 2. It is a multi-level quantum mechanical system coupled to a massless conformally coupled scalar field via the interaction Hamiltonian

$$H_{\text{int}} = cm(\tau)\phi(\tau) . \quad (152)$$

We consider a detector following the trajectory  $t = \tau$  that is  $\eta = -\alpha e^{-\tau/\alpha}$  and  $\mathbf{x} = 0$ . In (152) we consider the field smeared with a detector profile function over constant  $\tau$  hypersurfaces, that is

$$\phi(\tau) = \int d^3x W_\epsilon(\mathbf{x})\phi(\tau, \mathbf{x}) . \quad (153)$$

For the profile function we choose

$$W_\epsilon(\mathbf{x}) = \frac{1}{\pi^2} \frac{\epsilon e^{-\tau/\alpha}}{(\mathbf{x}^2 + \epsilon^2 e^{-2\tau/\alpha})^2} . \quad (154)$$

The detector shape (154) is now time dependent! The reason for this is that we want a detector which is rigid in its rest frame. That is, we want a detector which is rigid with respect to proper distance and not comoving distance. The two distances are related by  $L_{\text{prop}} = e^{\tau/\alpha} L_{\text{comov}}$ . In (153) the integration is done over  $\mathbf{x}$ , which is a comoving coordinate, and using a time independent shape function there would mean that the detector is rigid with respect to comoving distance. It is a simple matter to show that a shape function which selects a distance scale  $L'$  may be obtained from one which selects a distance scale  $L$  by

$$W_{L'}(\mathbf{x}) = \frac{L^3}{L'^3} W_L\left(\frac{L}{L'}\mathbf{x}\right) . \quad (155)$$

If we write (154) now in terms of proper distance we find

$$W_{\epsilon_{\text{prop}}}(\xi) = \frac{1}{\pi^2} \frac{\epsilon_{\text{prop}}}{(\mathbf{x}^2 + \epsilon_{\text{prop}}^2)^2} , \quad (156)$$

and so in terms of proper distance (154) is a rigid shape in the sense that it is time independent. Using this shape function we find, using the mode expansion of  $\phi$ ,

$$\begin{aligned} \langle 0_E | \phi(\tau)\phi(\tau') | 0_E \rangle &= \frac{\eta\eta'}{(2\pi)^3\alpha^2} \int \frac{d^3k}{2\omega} \int d^3x W_\epsilon(\mathbf{x}) e^{-i(\omega\eta(\tau)-\mathbf{k}\cdot\mathbf{x})} \\ &\quad \times \int d^3x' W_\epsilon(\mathbf{x}') e^{i(\omega\eta(\tau')-\mathbf{k}\cdot\mathbf{x}')} . \end{aligned} \quad (157)$$

Further we find

$$\begin{aligned} \int d^3x W_\epsilon(\mathbf{x}) e^{-i(\omega\eta(\tau)-\mathbf{k}\cdot\mathbf{x})} &= e^{-i|\mathbf{k}|\eta(\tau)} e^{-\epsilon|\mathbf{k}|e^{-\tau/\alpha}} , \\ &= e^{-i|\mathbf{k}|\eta(\tau)} e^{-\epsilon|\mathbf{k}|\dot{\eta}(\tau)} , \end{aligned} \quad (158)$$

where the integration is done by transforming to spherical coordinates. Hence

$$\langle 0_E | \phi(\tau) \phi(\tau') | 0_E \rangle = \frac{\eta\eta'}{(2\pi)^3\alpha^2} \int \frac{d^3k}{2\omega} e^{-i\omega(\eta-\eta'-i\epsilon(\dot{\eta}+\dot{\eta}'))} . \quad (159)$$

The expression (159) agrees with that found above from the ultraviolet cut-off regularization.

## 7.2 $\mathbb{RP}^3$ de Sitter space

In this section we consider an inertial detector that is linearly coupled to a conformally coupled massless scalar field in  $\mathbb{RP}^3$  de Sitter spacetime [11].<sup>5</sup>

$\mathbb{RP}^3$  de Sitter space is built as a quotient of de Sitter space under the group generated by the discrete isometry

$$J : (z_0, z_1, z_2, z_3, z_4) \mapsto (z_0, -z_1, -z_2, -z_3, -z_4) , \quad (160)$$

which induces a map  $\tilde{J}$  on the hyperboloid (136). Although  $J$  has fixed points on  $M$ ,  $\tilde{J}$  acts freely on the hyperboloid. The isometry group of four-dimensional de Sitter space is  $O(1, 4)$ , being the largest subgroup of the isometry group of the five-dimensional Minkowski embedding space which preserves (136). The isometry group of  $\mathbb{RP}^3$  de Sitter space is then the largest subgroup of  $O(1, 4)$  which commutes with  $J$ . That is,  $\mathbb{Z}_2 \times O(4)/\mathbb{Z}_2$  where the non-trivial element of the first  $\mathbb{Z}_2$  factor sends  $z_0$  to  $-z_0$  while the non-trivial element of the  $\mathbb{Z}_2$  in the second factor is given by  $J$  which clearly acts trivially on  $\mathbb{RP}^3$  de Sitter space. The connected component of the isometry group is  $SO(4)$ . The foliation given by  $z_0 = \text{constant}$  hypersurfaces is a geometrically distinguished one as it is the only foliation whose spacelike hypersurfaces are orbits of the connected component of the isometry group. This is made clearer by introducing the globally defined coordinates  $(t, \chi, \theta, \phi)$

$$\begin{aligned} z_0 &= \alpha \sinh(t/\alpha) , \\ z_4 &= \alpha \cosh(t/\alpha) \cos \chi , \\ z_1 &= \alpha \cosh(t/\alpha) \sin \chi \cos \theta , \\ z_2 &= \alpha \cosh(t/\alpha) \sin \chi \sin \theta \cos \phi , \\ z_3 &= \alpha \cosh(t/\alpha) \sin \chi \sin \theta \sin \phi , \end{aligned} \quad (161)$$

in which the metric reads

$$ds^2 = dt^2 - \alpha^2 \cosh^2(t/\alpha) [d\chi^2 + \sin^2 \chi (d\theta^2 + \sin^2 \theta d\phi^2)] , \quad (162)$$

where  $(\chi, \theta, \phi)$  on de Sitter ( $\mathbb{RP}^3$  de Sitter) space are a set of hyperspherical coordinates on  $S^3$  ( $\mathbb{RP}^3$ ) respectively.  $(t, \chi, \theta, \phi)$  make manifest the  $O(4)$  isometry subgroup.

---

<sup>5</sup>See also [56] for a nice discussion on de Sitter space vs  $\mathbb{RP}^3$  de Sitter.

We denote by  $|0_G\rangle$  the vacuum state induced by the Euclidean vacuum  $|0_E\rangle$  on de Sitter space (see [11] for more details). We consider a particle detector that is linearly coupled to a massless conformally coupled scalar field. The detector and field are assumed to be in the states  $|E_0\rangle$  and  $|0_G\rangle$  respectively at time  $\tau_0 = -\infty$ , and we seek the probability that at time  $\tau > \tau_0$  the detector is found in the state  $|E_1\rangle$ . Through arguments analogous to those in section 2, the transition rate is

$$\dot{F}_\tau(\omega) = 2 \int_0^\infty ds \operatorname{Re} (e^{-i\omega s} \langle 0_G | \phi(\tau) \phi(\tau - s) | 0_G \rangle) . \quad (163)$$

By the method of images we have

$$\langle 0_G | \phi(x) \phi(x') | 0_G \rangle = \langle 0_E | \phi(x) \phi(x') | 0_E \rangle + \langle 0_E | \phi(x) \phi(Jx') | 0_E \rangle , \quad (164)$$

where on the RHS expressions live in de Sitter space, and the correlation function  $\langle 0_E | \phi(x) \phi(x') | 0_E \rangle$  is given by (146).

Consider now a detector that follows the geodesic worldline

$$\begin{aligned} z_0 &= \alpha \sinh(\tau/\alpha) , \\ z_4 &= \alpha \cosh(\tau/\alpha) , \\ z_1 = z_2 = z_3 &= 0 . \end{aligned} \quad (165)$$

On  $\mathbb{RP}^3$  de Sitter space this represents the motion of any geodesic observer whose motion is orthogonal to the distinguished foliation. The transition rate (163) is in two parts, a de Sitter part and an image part. We have calculated already the de Sitter part, coming from the first term in (164), in section 7.1. The result was the usual thermal, Planckian, response at temperature  $T = 1/(2\pi\alpha)$ . We need the image term. In order to find  $\langle 0_E | \phi(x) \phi(Jx') | 0_E \rangle$  on this worldline we first write  $\langle 0_E | \phi(x) \phi(x') | 0_E \rangle$  in terms of the coordinates  $(z_0, z_1, z_2, z_3, z_4)$  of the embedding space and then act on  $x'$  with  $J$ , finding

$$\langle 0_E | \phi(x) \phi(Jx') | 0_E \rangle = \frac{1}{8\pi^2} \frac{1}{(+\mathbf{z} \cdot \mathbf{z}' + z_0 z'_0 + \alpha^2)} , \quad (166)$$

where  $\mathbf{z} = (z_1, z_2, z_3, z_4)$ . The regularization has been omitted as the worldline and its image under  $J$  are completely spacelike separated. The image term gives to the transition rate the contribution

$$\dot{F}_{I\tau}(\omega) = 2 \int_0^\infty ds \frac{\cos(\omega s)}{16\pi^2 \alpha^2 \cosh^2(\frac{2\tau-s}{2\alpha})} . \quad (167)$$

We see that the image term contribution (167) is exactly the same as the image term contribution in the response of a uniformly accelerated detector on a four-dimensional Minkowski space with boundary at  $x = 0$  ((55) with  $d = 4$ ). Therefore the total response of our inertial detector in  $\mathbb{RP}^3$  de Sitter space (with Ricci scalar  $R = 12/\alpha^2$ ) is identical to the response of a uniformly accelerated detector travelling in four-dimensional Minkowski space with a boundary at  $x = 0$  with the acceleration  $1/\alpha$  perpendicular to the boundary. It follows that our numerical results in figure 4 also give the response on  $\mathbb{RP}^3$  de Sitter space, with the appropriate interpretation for  $\alpha$ . In particular, the image term breaks the KMS condition and the response is

non-thermal and non-Planckian. When the detector is switched on in the infinite past, the response at large  $\tau$  is oscillatory in  $\tau$  with period  $\pi/\omega$ . When the detector is switched on at a finite time  $\tau_0$ ,  $\tau_0 \ll -1$ , numerical evidence indicates that the response is approximately periodic in the region  $0 < \tau < -\tau_0$ , with period  $\pi/\omega$ , but it falls to the thermal response as  $\tau \rightarrow \infty$ , as discussed further in section 4.2 and illustrated in figures 5, 6 and 7. This clarifies and adds to the discussion given in [11].

We wish to compare these particle detector results in  $\mathbb{RP}^3$  de Sitter space to the associated GEMS particle detector. We see from (165) that the GEMS worldline of interest is a Rindler trajectory with acceleration  $a = 1/\alpha$  in the 5-dimensional embedding space. Therefore in the 5-dimensional Minkowski embedding space of de Sitter space we see that the response of a detector following this worldline is a thermal one with associated temperature  $T = 1/(2\pi\alpha)$  and so we expect, as indeed we saw in section 7.1, the response of the detector in de Sitter space to also be a thermal one with temperature  $T = 1/(2\pi\alpha)$ . Again the actual responses of detectors in the two situations are not identical (as seen in sections 2 and 7.1) due to the different dimensions of the spaces, the most obvious difference being the presence of the Planckian factor in the de Sitter response and the Fermi factor in Rindler response on the odd dimensional embedding space. As the  $\mathbb{RP}^3$  de Sitter spacetime is built as a quotient of de Sitter space under the map  $J : (z_0, z_1, z_2, z_3, z_4) \mapsto (z_0, -z_1, -z_2, -z_3, -z_4)$  we have immediately the action of this map on the embedding space. The geodesic worldline of interest maps to a Rindler worldline in this embedding space with acceleration  $a = 1/\alpha$ , so in the GEMS approach we consider a Rindler particle detector with this acceleration in this 5-dimensional embedding space. The transition rate was found in section 4.3. The thermal part of the transition rate is constant in time and is given by

$$\dot{F}_{M\tau}(\omega) = \frac{a^2}{8\pi(e^{\frac{2\pi\omega}{a}} + 1)}(1/4 + \omega^2/a^2), \quad (168)$$

corresponding to the temperature  $T = \frac{a}{2\pi}$ . The image part of the transition rate depends on the proper time and is given by

$$\dot{F}_{I\tau}(\omega) = \frac{1}{4\pi^2} \int_0^\infty ds \frac{\cos(\omega s)}{\left(4/a^2 \cosh^2\left(\frac{a(2\tau-s)}{2}\right)\right)^{3/2}}. \quad (169)$$

The total response is shown for various values of the parameters in figure 9. The qualitative similarities to the  $\mathbb{RP}^3$  de Sitter transition rate are apparent. They provide evidence that, at least in some cases, the GEMS procedure may be applied to quotient spaces such as  $\mathbb{RP}^3$  de Sitter space and the  $\mathbb{RP}^3$  geon where the embedding spaces are Minkowski spaces with suitable identifications.

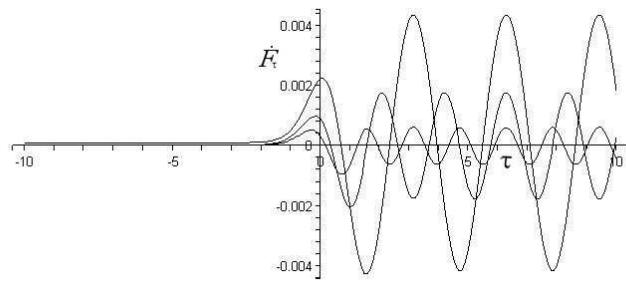


Figure 9: Transition rate for a detector uniformly accelerated in the  $z_1$  direction on the quotient space of 5-dimensional Minkowski space under the involution  $J$ . The parameters are  $\alpha = 1$ ,  $C = (2z_1)^2 + (2z_2)^2 + (2z_3)^2 = 0$  and  $\omega = 1$  (upper curve),  $\omega = 1.5$  and  $\omega = 2$  (lower curve).

## 8 Discussion

In this paper we considered particle detector models in the context of quantum field theory in curved spacetime. In particular we investigated the model of Schlicht [1]. The model is that of a monopole detector linearly coupled to a massless scalar field which is smeared with a window function in order to regularize the correlation function in the transition rate. We extended the regularization of the correlation function for the massless linearly coupled scalar field to  $d$ -dimensional Minkowski space, and we showed that it leads to the expected responses for inertial and uniformly accelerated detectors switched on in the infinite past and off at  $\tau < \infty$ . Further we extended the regularization of Schlicht to the massive scalar field in Minkowski space and have shown that it reduces to that of [1] in the massless limit.

Next we introduced a model of a linearly coupled massless scalar field detector on spacetimes built as quotients of Minkowski space under certain discrete isometries. In a number of cases the model, when switched on at  $\tau_0 = -\infty$  and read at  $\tau < \infty$ , was shown to reproduce the known asymptotic responses. These cases include the uniformly accelerated detector on  $M_0$  [9, 33] as well as the inertial and uniformly accelerated detectors on Minkowski space with boundary when the motion is parallel to the boundary [33]. These results suggest that our model is reasonable. Further we presented a number of new responses, the most interesting of which are the time dependent responses on Minkowski space with boundary and on  $M_-$ . An inertial detector approaching the boundary on Minkowski space with boundary was seen to react in a qualitatively similar way to one travelling parallel to the boundary but taking progressively smaller distances (ie comparing figures 1 and 3). The main difference is that in the detector approaching the boundary a divergence in the transition rate occurs as the boundary is reached. A detector with uniform acceleration perpendicular to the boundary was also considered, the results were seen to be more subtle and an interesting observation made. For a detector which is switched on in the infinite past the transition rate is found to oscillate in  $\tau$  at late times with period  $\pi/\omega$ , never tending to the Minkowski thermal response, no matter how far from the boundary the detector gets in the future. However for a detector switched on at a finite time (that is  $\tau_0 > -\infty$ ), the response will at late times tend to the thermal Minkowski response. For instantaneous, exponential and Gaussian switching functions the conclusion is the same.

Responses were also considered on the quotient spaces of Minkowski space under the involution  $J_{c_k} : (t, x_1, x_2, \dots, x_{d-1}) \mapsto (t, -x_1, -x_2, -\dots - x_k, x_{k+1}, \dots, x_{d-1})$  where  $1 < k < d$  and certain relations to the responses on Minkowski space with boundary noted. The responses are relevant for discussions of detectors in the spacetime outside an infinitely long and zero radius cosmic string. The responses of uniformly accelerated detectors, where the motion is in the  $x_1$  direction, are also relevant for the discussion of static detectors in the  $\mathbb{RP}^3$  geon exterior as well as co-moving detectors in  $\mathbb{RP}^3$  de Sitter via their global embedding Minkowski spacetimes (GEMS).

Next we extended the detector model and regularization to the massless Dirac field. With a few minor technicalities the extension is quite straightforward. The transition rate and the power spectrum of the Dirac noise for a detector switched on in the infinite past on inertial and a uniformly accelerated trajectories was obtained.

The power spectrum for the accelerated detector agrees with the previous literature (see e.g [6]) and so suggests our model is reasonable. Further we briefly considered the response of the Dirac detector on  $M_0$  and  $M_-$ . One aim was to see whether a uniformly accelerated Dirac detector on  $M_-$  could distinguish the two spin structures there. We found this not to be the case for our detector model.

In section 6 we considered the response of a static detector in the exterior region of the  $\mathbb{RP}^3$  geon via a global embedding Minkowski space. Although the GEMS programme has so far only been applied in a kinematical setting, our aim was to examine the possibility that the response of the detector in the embedding space is related to that in the underlying curved space and further whether the GEMS scheme can be applied to quotient spaces, such as the  $\mathbb{RP}^3$  geon and  $\mathbb{RP}^3$  de Sitter space, where the embedding spaces are Minkowski spaces with suitable identifications. We found that the response is related to that of uniformly accelerated detectors given in section 4.3. In particular it is shown in the embedding space, and expected on the geon, that the response is not thermal, in the sense that it does not satisfy the KMS condition, for most times. Further it is seen that for a detector switched on in the infinite past the response is approximately thermal at early times but does not return to the thermal response at late times in contrast to expectations (see e.g [9, 10]). If the detector however is turned on at some finite time in the distant past then the response is approximately thermal when turned on and returns to being approximately thermal in the distant future.

Lastly we considered some responses on de Sitter space and  $\mathbb{RP}^3$  de Sitter space. The regularization of [1] is not easily adaptable to general motions in these spacetimes, due to the possibility of spatially closed hypersurfaces in the detector's rest frame. We argued however for a similar regularization by reinterpreting the regularization as an ultraviolet cut-off in the high "frequency" modes. On de Sitter space the transition rate for a detector switched on in the infinite past is found for a uniformly accelerated detector, and it is found to agree with previous literature [26]. This result suggests our regularization is reasonable. In the case of an inertial detector in de Sitter space the regularization we introduced is shown to also come from the consideration of a detector with spatial extension where the detector is rigid in its rest frame. On  $\mathbb{RP}^3$  de Sitter space the response of a detector following the comoving worldline was considered in two ways. Firstly a direct calculation showed that the response is exactly that of a uniformly accelerated detector approaching the boundary on Minkowski space with boundary (identifying  $1/\alpha$  with the acceleration). Again therefore the response of a detector switched on in the infinite past has an oscillatory behaviour in the distant future and does not tend to the expected thermal result, the image term breaking the KMS condition, in contrast to what was expected [11]. The response of a detector switched on at a finite time does however tend to the expected thermal response at late times. Secondly we considered the same calculation from the GEMS perspective. Although the response is clearly different to that in the original space, due to the different dimensions of  $\mathbb{RP}^3$  de Sitter space and the embedding space, it is seen that the response is qualitatively very similar. The calculation therefore provides a good example for investigating the relation between detector responses in curved spacetimes and those in their GEMS, and the use of the GEMS procedure on such quotient spaces where the embedding spaces are Minkowski spaces with suitable identifications. The calculation further

suggests that the response found in the GEMS of the  $\mathbb{RP}^3$  geon in section 6 is indeed closely related to the response of the static detector in the geon itself.

### Acknowledgements

I would like to thank Jorma Louko for many useful discussions and for reading the manuscript. This work was supported by the University of Nottingham and the States of Guernsey Education Department.

## References

- [1] S. Schlicht, *Class.Quant.Grav* **21**, 4647 (2004) [⟨arXiv:gr-qc/0306022⟩](https://arxiv.org/abs/gr-qc/0306022)
- [2] N. D. Birrell and P. C. W. Davies, “*Quantum Fields in Curved Space*” Cambridge University Press (Cambridge, 1982)
- [3] W. G. Unruh, *Phys.Rev.D* **14**, 870 (1976)
- [4] S. W. Hawking, *Commun.Math.Phys* **43**, 199 (1975)
- [5] B. S. DeWitt, “*Quantum gravity: the new synthesis*” in “*General Relativity and Einstein centenary survey*” ed S. W. Hawking, W. Israel, Cambridge University Press (Cambridge, 1979)
- [6] S. Takagi, *Prog.Theor.Phys.Supp* **88**, 1 (1986)
- [7] R. Banach and J. S. Dowker, *J.Phys.A:Math.Gen* **12**, 2527 (1979)
- [8] R. Banach and J. S. Dowker, *J.Phys.A:Math.Gen* **12**, 2545 (1979)
- [9] J. Louko and D. Marolf, *Phys.Rev.D* **58**, 024007 (1998) [⟨arXiv:gr-qc/9802068⟩](https://arxiv.org/abs/gr-qc/9802068)
- [10] P. Langlois, *Phys.Rev.D* **70**, 104008 (2004) [⟨arXiv:gr-qc/0403011⟩](https://arxiv.org/abs/gr-qc/0403011)
- [11] J. Louko and K. Schleich, *Class.Quant.Grav* **16**, 2005 (1999) [⟨arXiv:gr-qc/9812056⟩](https://arxiv.org/abs/gr-qc/9812056)
- [12] P. C. W. Davies and A. C. Ottewill, *Phys.Rev.D* **65**, 104014 (2002) [⟨arXiv:gr-qc/0203003⟩](https://arxiv.org/abs/gr-qc/0203003)
- [13] L. H. Ford, *Phys.Rev.D* **43**, 3972 (1991)
- [14] L. H. Ford and T. A. Roman, *Phys.Rev.D* **55**, 2082 (1997) [⟨arXiv:gr-qc/9607003⟩](https://arxiv.org/abs/gr-qc/9607003)
- [15] M. J. Pfenning and L. H. Ford, *Phys.Rev.D* **55**, 4813 (1997) [⟨arXiv:gr-qc/9608005⟩](https://arxiv.org/abs/gr-qc/9608005)
- [16] M. J. Pfenning and L. H. Ford, *Phys.Rev.D* **57**, 3489 (1998) [⟨arXiv:gr-qc/9710055⟩](https://arxiv.org/abs/gr-qc/9710055)

- [17] L. H. Ford, M. J. Pfenning and T. A. Roman, Phys.Rev.D **57**, 4839 (1998) [⟨arXiv:gr-qc/9711030⟩](https://arxiv.org/abs/gr-qc/9711030)
- [18] C. J. Fewster and S. P. Eveson, Phys.Rev.D **58**, 084010 (1998) [⟨arXiv:gr-qc/9805024⟩](https://arxiv.org/abs/gr-qc/9805024)
- [19] C. J. Fewster and E. Teo, Phys.Rev.D **59**, 104016 (1999) [⟨arXiv:gr-qc/9812032⟩](https://arxiv.org/abs/gr-qc/9812032)
- [20] C. J. Fewster, Class.Quant.Grav **17**, 1897 (2000) [⟨arXiv:gr-qc/9910060⟩](https://arxiv.org/abs/gr-qc/9910060)
- [21] L. H. Ford, N. F. Svaiter and M. L. Lyra, Phys.Rev.A **49**, 1378 (1994)
- [22] B. F. Svaiter and N. F. Svaiter, Class.Quant.Grav **11**, 347 (1994)
- [23] P. C. W. Davies and V. Sahni, Class.Quant.Grav **5**, 1 (1988)
- [24] S. Deser and O. Levin, Phys.Rev.D **59**, 064004 (1999) [⟨arXiv:hep-th/9809159⟩](https://arxiv.org/abs/hep-th/9809159)
- [25] A. Chamblin and G. W. Gibbons, Phys.Rev.D **55**, 2177 (1997)
- [26] S. Deser and O. Levin, Class.Quant.Grav **14**, L163 (1997) [⟨arXiv:gr-qc/9706018⟩](https://arxiv.org/abs/gr-qc/9706018)
- [27] A. S. Wightman, in “*1964 Cargese Lectures in Theoretical Physics*” ed M. Levy, Gordon and Breach (1967)
- [28] C. W. Misner, K. S. Thorne and J. A. Wheeler, “*Gravitation*” Freeman (New York 1973)
- [29] L. Sriramkumar, Mod.Phys.Lett **A17**, 1059 (2002) [⟨arXiv:gr-qc/0206048⟩](https://arxiv.org/abs/gr-qc/0206048)
- [30] I. S. Gradshteyn and I. M. Ryzhik, “*Table of Integrals Series and Products*” Academic Press (2000)
- [31] P. Langlois, Class.Quant.Grav **22**, 4141 (2005) [⟨arXiv:gr-qc/0504121⟩](https://arxiv.org/abs/gr-qc/0504121)
- [32] D. Zwillinger, “*CRC Standard Mathematical Tables and Formulae*” Chapman and Hall/CRC Press LLC (2003)
- [33] P. C. W. Davies, Z. X. Liu and A. C. Ottewill, Class.Quant.Grav **6**, 1041 (1989)
- [34] N. Suzuki, Class.Quant.Grav **14**, 3149 (1997)
- [35] M. Abramowitz and I. A. Stegun, “*Handbook of Mathematical Functions*” Dover Publications, Inc (New York, 1970)
- [36] B. F. Svaiter and N. F. Svaiter, Phys.Rev.D **46**, 5267 (1992) Erratum, Phys.Rev.D **47**, 4802 (1993)
- [37] A. Higuchi, G. E. A. Matsas and C. B. Peres, Phys.Rev.D **48**, 3731 (1993)
- [38] L. Sriramkumar and T. Padmanabhan, Class.Quant.Grav **13**, 2061 (1996)

- [39] K. Schleich and D. M. Witt Nucl.Phys.B **402**, 411 (1993) [⟨arXiv:gr-qc/9307015⟩](https://arxiv.org/abs/gr-qc/9307015)
- [40] K. Schleich and D. M. Witt Nucl.Phys.B **402**, 469 (1993) [⟨arXiv:gr-qc/9307019⟩](https://arxiv.org/abs/gr-qc/9307019)
- [41] R. P. Geroch and J. Traschen, Phys.Rev.D **36**, 1017 (1987)
- [42] D. Garfinkle, Class.Quant.Grav **16**, 4101 (1999) [⟨arXiv:gr-qc/9906053⟩](https://arxiv.org/abs/gr-qc/9906053)
- [43] A. Vilenkin, Phys.Rev.D **23**, 852 (1981)
- [44] M. R. Anderson, “*The mathematical theory of cosmic strings*” IOP Publishing (2003)
- [45] S. Deser and O. Levin, Class.Quant.Grav **15**, L85 (1998) [⟨arXiv:hep-th/9806223⟩](https://arxiv.org/abs/hep-th/9806223)
- [46] H. F Goenner in “*General Relativity and Gravitation*” Plenum Press (New York 1980)
- [47] N. L. Santos, O. J. C. Dias and J. P. S. Lemos, Phys.Rev.D **70**, 124033 (2004) [⟨arXiv:hep-th/0412076⟩](https://arxiv.org/abs/hep-th/0412076)
- [48] Y. Kim, Y. Park and K. Soh, Phys.Rev.D **62**, 104020 (2000) [⟨arXiv:gr-qc/0001045⟩](https://arxiv.org/abs/gr-qc/0001045)
- [49] S. Hong, Y. Kim, and Y. Park, Phys.Rev.D **62**, 024024 (2000) [⟨arXiv:gr-qc/0003097⟩](https://arxiv.org/abs/gr-qc/0003097)
- [50] S. Hong, W. Kim, Y. Kim, and Y. Park, Phys.Rev.D **62**, 064021 (2000) [⟨arXiv:gr-qc/0006025⟩](https://arxiv.org/abs/gr-qc/0006025)
- [51] S. Hong, W. Kim, J. Oh and Y. Park, Phys.Rev.D **63**, 127502 (2001) [⟨arXiv:hep-th/0103036⟩](https://arxiv.org/abs/hep-th/0103036)
- [52] S. Hong, W. Kim, J. Oh and Y. Park, J.Korean.Phys.Soc **42**, 23 (2003) [⟨arXiv:gr-qc/0110057⟩](https://arxiv.org/abs/gr-qc/0110057)
- [53] H. Chen and Y. Tian, Phys.Rev.D **71**, 104008 (2005)
- [54] C. Fronsdal, Phys.Rev **116**, 778 (1959)
- [55] B. Allen, Phys.Rev.D **32**, 3136 (1985)
- [56] B. McInnes, J.High Energy.Phys JHEP 09(2003)009, (2003) [⟨arXiv:hep-th/0308022⟩](https://arxiv.org/abs/hep-th/0308022)